Energy Reviews 3 (2024) 100099

Contents lists available at ScienceDirect

Energy Reviews

journal homepage: www.journals.elsevier.com/energy-reviews

Full Review Article

Flexible fuel cells: A prospective review

Yifei Wang [a], Xinhai Xu [a], Guangzhong Dong [a], Mingming Zhang [a,*], Kui Jiao [b,**], Dennis Y.C. Leung [c,***]

[a] School of Mechanical Engineering and Automation, Harbin Institute of Technology, Shenzhen, China
[b] State Key Laboratory of Engines, Tianjin University, Tianjin, China
[c] Department of Mechanical Engineering, The University of Hong Kong, Hong Kong, China

ARTICLE INFO

Keywords:
Flexible fuel cell
Polymer electrolyte membrane fuel cell
Membraneless fuel cell
Biofuel cell
Wearable electronics

ABSTRACT

With the widespread of wearable electronics in healthcare, military and entertainment sectors, flexible power sources have attracted great attention, among which flexible fuel cells are relatively young compared with flexible batteries, supercapacitors and energy harvesters. Fuel cell is well known for its uninterrupted operation, high energy density and instant refueling ability, which is especially advantageous for long-term and outdoor missions. To date, existing flexible fuel cell studies can be classified into three major types based on their electrolyte and catalyst material, namely the flexible polymer electrolyte membrane fuel cell (PEMFC), membraneless fuel cell (MFC) and biofuel cell (BFC). The flexible PEMFC generally employs hydrogen as fuel so that a power density of hundreds of mW cm^{-2} can be achieved. Relevant research efforts are mainly paid to the replacement of conventional rigid cell components with flexible substitutes. Moreover, novel cell structures such as ultrathin cell and tubular cell have also been proposed. However, the flexible hydrogen storage is still a research gap. The flexible MFC has a much wider choice of fuel such as methanol, ethanol and formate, but the power output is limited to dozens of mW cm^{-2} due to more sluggish fuel oxidation. To circumvent the demand of pumping, porous materials with capillary action are preferred as cell substrate, such as cellulose paper and cotton thread, which can absorb electrolyte solution passively. Nevertheless, the capillary flow rate is not controllable at the moment. As for the flexible BFC, it is primarily targeted for epidermal applications in order to utilize natural organic materials in human body fluid. Benefited from this, the flexible BFC can have the simplest cell structure of two bioelectrodes only, which can be integrated onto contact lenses, tattoos, clothes, etc. However, the complex organic fuel oxidation as well as the mild electrolyte pH have greatly restricted its power density to μW cm^{-2} level. In this work, a comprehensive review on existing flexible fuel cell studies is provided, including cell structure, material, performance together with their advantages and disadvantages. Based on this, solid conclusions are made on their development trend and future perspectives are presented as well.

1. Introduction

Fuel cell is an electrochemical energy conversion device which can produce electricity directly from various fuels including hydrogen, hydrogen peroxide, hydrocarbons, nitrogenous compounds, etc., with the help of an oxidant such as ambient air. Similar to batteries, a fuel cell works by separating a pair of redox reaction into independent anodic oxidation and cathodic reduction, whose core component is also an electrolyte layer sandwiched by two electrodes. As shown in Fig. 1a, the fuel is oxidized at anode to give free electrons while the oxidant is reduced at cathode to accept them, leading to electricity generation during electron exchange in the external circuit [1]. Specifically, one distinct advantage of fuel cell is its long-term and uninterrupted operation ability as long as fuel and oxidant are supplied, while the battery electricity is generally limited and needs to be replaced (primary) or recharged (secondary) periodically. In addition, fuel cell is also famous for its excellent energy density, especially in long-term missions where the fuel weight is significantly higher than the cell itself. Furthermore, fuel cell can be highly clean and carbon-neutral when renewable fuels such as green hydrogen and bioethanol are employed, which is also

* Corresponding author.
** Corresponding author.
*** Corresponding author.
E-mail addresses: mmzhang@hit.edu.cn (M. Zhang), kjiao@tju.edu.cn (K. Jiao), ycleung@hku.hk (D.Y.C. Leung).

https://doi.org/10.1016/j.enrev.2024.100099
Received 8 January 2024; Received in revised form 23 May 2024; Accepted 8 June 2024

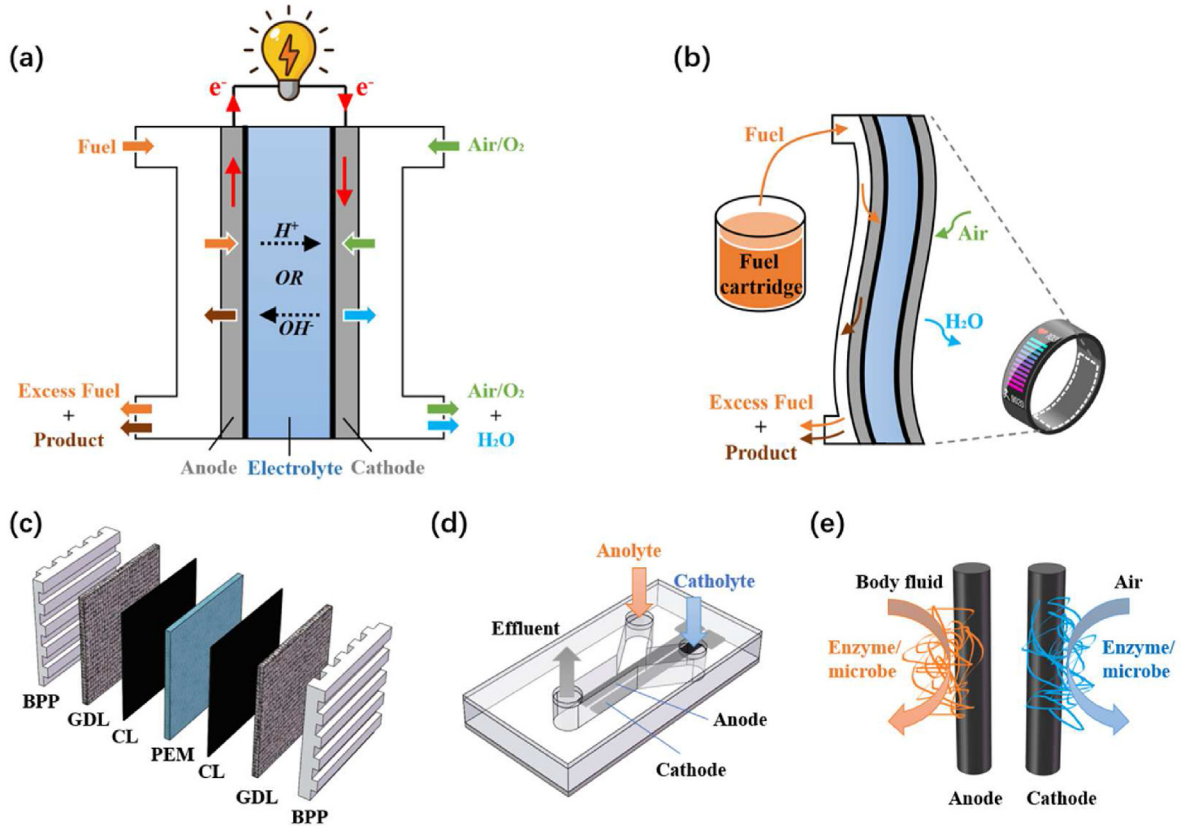

Fig. 1. Classification of FFCs according to their electrode/electrolyte materials: (a) General working principle of conventional rigid fuel cell; (b) Schematic diagram of a typical FFC; (c) Typical PEMFC; (d) Typical MFC; (e) Typical BFC.

energy-efficient and noise-free during operation. Regarding all these merits, great R&D efforts have been made to this technology during the last century, pushing its real application in the field of aerospace mission, military equipment, stationary power station and electric vehicles [2]. However, the market share is still much lower than other energy conversion technologies at present, which is mainly due to its relatively high cost, unsatisfactory long-term durability and perhaps the safety concerns related to hydrogen gas.

Recently, flexible electronics are getting more and more attention because of their tremendous prospect in wearable applications, ranging from ubiquitous healthcare, wearable equipment to personal entertainment, promising a huge market in the near future [3]. Regarding this trend, the development of flexible power sources for them is of vital importance, which should be bendable, stretchable, lightweight, together with high energy density and device safety [4]. Till now, some flexible power sources have already been found in the niche market, such as the primary dry battery and the secondary Li ion battery. In addition, new technologies with different energy generation mechanisms are also under extensive investigation, such as non-Li ion batteries [5], metal-air batteries [6], supercapacitors [7], and various energy harvesters from solar [8], thermal [9], mechanical [10] and radiofrequency energies [11]. Benefited from their relatively low self-discharge and high energy density, flexible batteries are able to function independently in the wearable electronic system, but they need to be replaced or recharged periodically which causes either system interruption or user inconvenience. On the contrary, the flexible supercapacitor allows fast recharge but has a relatively high self-discharge rate, which is not convenient as well for long-term missions. As for energy harvesters, they are generally combined with batteries or supercapacitors in order to achieve a stable output, leading to a more complex energy system with reduced energy density. These demerits are generally insignificant for applications with intermittent usage, such as wearable equipment and personal entertainment. However, the continuous operation ability and high energy density are of key importance to the wearable healthcare system, such as the wireless body sensor network, which has to be worn and functioned continuously for a long period of time regardless of the ambient environment [12]. Considering this specific requirement, the flexible fuel cell with uninterrupted operation ability can be a more appropriate solution as shown in Fig. 1b. In general, soft, thin and lightweight materials need to be utilized for all cell components in order to achieve certain flexibility, including the electrodes, electrolyte and reactant channel. For the cathode side, an air-breathing configuration is preferred for system simplification. As for the anode side, a fuel cartridge can be used to support its continuous discharge, which is replaceable instantly before the fuel inside is exhausted. The fundamental working principle is basically the same with rigid fuel cells. However, considering the frequent deformation in wearable applications, key R&D issues of flexible fuel cell lie in its discharge stability due to components' delamination and long-term durability due to microstructure collapse.

Flexible fuel cell (FFC) is a young technology which was first proposed in the early 21st century [13]. It is mainly targeted for powering wearable electronics either integrated in the clothes or attached on the skin directly. Based on their electrolyte/electrode material, the FFC studies in literature can be roughly divided into three groups, namely the polymer electrolyte membrane fuel cell (PEMFC), the membraneless fuel cell (MFC) and the biofuel cell (BFC). As shown in Fig. 1c, the PEMFC is mainly composed of a membrane electrolyte, two catalyst layers, two gas diffusion layers (GDL) and two bipolar plates (BPP). It can provide a relatively high power density of several hundred mW cm^{-2} at room temperature using hydrogen as fuel, which is made flexible by replacing the conventional rigid GDL and BPP with flexible materials. However, the fabrication cost is relatively high due to the expensive membrane electrolyte and complex system [14]. Regarding this, the MFC shown in Fig. 1d eliminates the membrane electrolyte and uses microfluidic

electrolytes instead, which are flowed between electrodes by either active pumping or capillary action [15]. Liquid fuels such as alcohol, formate and hydrogen peroxide are more favored than hydrogen gas, leading to a lower power density of dozens of mW cm^{-2}. Both of the above two cases employ abiotic catalysts such as noble metals and non-noble metal oxides to ensure a satisfactory power output, while the BFC shown in Fig. 1e chooses to use enzymes or microbes as bio-catalysts, which is mainly targeted for harvesting energy from body secretions such as sweat, tear and urine [16]. However, the power density is much lower due to the slow reaction kinetics and mild electrolyte pH, ranging from several to several hundred μW/cm^2. In addition to this classification from material aspect, the FFC can also be divided into planar and tubular cells based on their structure, of which the former is used in conformal situations while the latter is targeted for weaving into clothes. Furthermore, from the fueling mode point of view, some FFCs employ a replaceable fuel cartridge to ensure a continuous and stable operation, while others receive fuel intermittently either from external supply or from the human body. In this review, we choose to group the FFC studies based on their materials, while the structure and fueling features are specified as well in corresponding sections for better comparison purpose.

The FFC technology has already been studied for nearly two decades with fruitful discoveries and outcomes. Nevertheless, a comprehensive review with future perspectives is still missing. Bandodkar et al. [16] and Huang et al. [17] summarized the research progress of wearable BFC only, Haque et al. [18] studied the recent advancement of wearable enzymatic fuel cell only, and Duan et al. [19] reviewed the flexible PEMFC only. Recently, Yang et al. [20] published a brief report on FFCs including BFCs, PEMFCs, solid oxide fuel cells (SOFC) and direct liquid fuel cells, but the content is quite limited with only a portion of related papers (less than 30). Wang et al. [21] summarized wearable fuel cells from the perspective of cell structure, regardless of the nature of different fuel cell types. Herein, we aim to give a more comprehensive and detailed review on FFCs from its very beginning, including flexible PEMFCs, MFCs, BFCs, SOFCs, photocatalytic fuel cells and liquid metal fuel cells. The review structure is arranged as follow: Section-2 focuses on flexible PEMFCs with soft GDLs and BPPs, adopting either Nafion membrane or polymer gel as electrolyte. Section-3 summarizes flexible MFCs built on different substrates, including polymer film, cellulose paper and cotton thread. Section-4 introduces flexible BFCs separately based on the nature of biocatalyst, namely the flexible enzymatic fuel cell and the flexible microbial fuel cell. As for other less studied cases such as flexible SOFCs, photocatalytic fuel cells and liquid metal fuel cells, they will be briefly introduced in Section-5. Finally, an overall summary and conclusion will be made on the existing FFC studies in Section-6, including their achievements and limitations. Potential solutions to these issues will be proposed as well for their future development.

2. Flexible PEMFCs

PEMFC is a predominant fuel cell technology working at relatively low temperature (generally below 100 °C for low-temperature PEMFC and between 120 and 200 °C for high-temperature PEMFC [22]), which has already been applied successfully in stationary power generation and electric vehicles. From the inmost to the outmost, a single cell is mainly composed of a PEM (mostly Nafion® membrane), two catalyst layers, two GDLs and two BPPs, which are generally stacked one on the top of the other with a planar structure as shown in Fig. 2a. Currently, great efforts have been devoted to this technology in order to push it further in the huge market, especially of electric vehicles, including the research on polymer membrane [23], catalyst material [24], catalyst layer design [25], GDL material and structure [26], BPP material and flow field [27], stacking strategies [28], systematic control [29], etc. As for flexible PEMFCs, since polymer membrane and catalyst layer are intrinsically flexible, the current research interest is mainly focused on finding soft materials for the GDL and BPP. Conventional carbon paper-based GDL is well known for its high electric conductivity and low cost, which is made of intertwined carbon fibers and binding polymers such as PTFE. In fact, the carbon paper can also be bent to certain extent, which is frequently adopted in flexible PEMFC studies. Alternatively, the carbon cloth woven with soft carbon fibers can be used instead which shows higher flexibility, but the electric conductivity is slightly lower. As for the BPP, conventional graphite and stainless-steel materials are both rigid as well as heavyweight. Therefore, flexible polymer materials with conductive coating are used instead, such as the Au/Ag-coated PDMS, while the serpentine flow channel can be fabricated by a simple hot-embossing technology [30]. In addition to the mainstream planar cell design, the tubular PEMFC with a cable shape has also been proposed in literature as shown in Fig. 2b, which was less studied due to its complicated fabrication process and lower modularity. Nevertheless, for wearable applications, a fine tubular PEMFC can be easily sewed into clothes or even woven into a complete fuel cell textile, which can obtain larger electrode area without undermining the user comfort level. In the following content, these two types of flexible PEMFCs will be introduced separately.

2.1. Planar cell design (hydrogen fuel)

For flexible PEMFCs with planar cell design, the conventional MEA with Nafion membrane and Pt catalyst is commonly adopted without any modification. Research emphasis is mainly put on developing flexible BPPs [31–40] and GDLs [41–46], while other novel cell structures were also proposed [13,47–50]. Most of these works employ hydrogen gas as fuel, ensuring a satisfactory power density around 100 mW/cm^2, but the long-term durability was rarely studied especially under repetitive

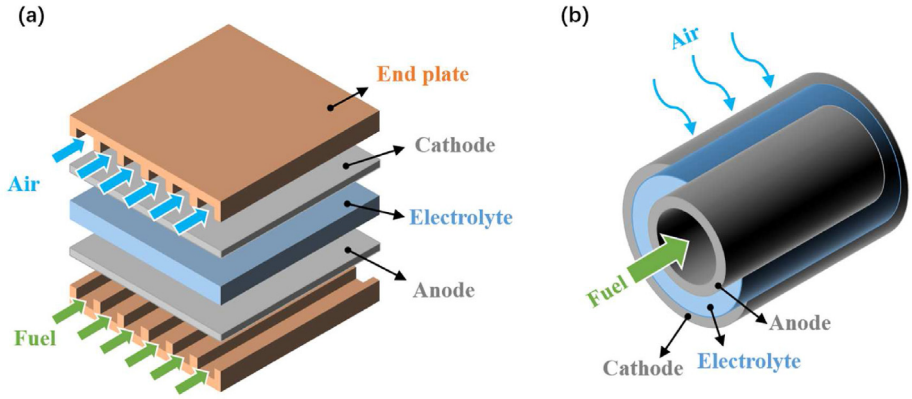

Fig. 2. Two major cell designs for flexible PEMFC: (a) Planar cell; (b) Tubular cell.

Table-1
Summary of flexible planar PEMFCs with hydrogen as fuel.

References	Fueling mode	GDL	BPP	OCV	Peak Power density	Long-term durability	Flexibility
Flexible BPP studies							
Wheldon et al. [31]	Flow & Play	C paper	Polyester	0.8 V	57 mW/cm^2		
Chang et al. [32]	Flow & Play	C paper	PDMS + Ni–Au film	1 V	20.5 mW/cm^2		Bending
Chang et al. [33]	Flow & Play	C paper	PDMS + Ag nanowire	1.04 V	71 mW/cm^2		Bending
Chang et al. [34]	Flow & Play	C paper	PDMS + Ag nanowire	1 V[a]	82 mW/cm^2		Bending
Chang et al. [35]	Flow & Play	C paper	PDMS + Ag nanowire	1 V[a]	117 mW/cm^2		Bending
Yoo et al. [38]	Flow & Play	C paper	PDMS (pre-bent)	1 V[a]	88.7 mW/cm^2		Bending
Yoo et al. [39]	Flow & Play	C paper	PDMS (3D printed)	0.9 V[a]	87.1 mW/cm^2	12 h (0.6 V)	Bending (200 times)
Park et al. [36]	Flow & Play	C paper	PDMS + Ag nanowire	0.95 V	110 mW/cm^2		
Park et al. [37]	Flow & Play	C paper	PDMS + Ag nanowire	0.91 V	26.8 mW/cm^2		Bending; Twisting
Baek et al. [40]	Flow & Play	C cloth	PDMS	0.85V[a]	36.6 mW/cm^2		Folding (300 times)
Flexible GDL studies							
Kang et al. [41]	Flow & Play	C cloth	PDMS	0.89 V	43 mW/cm^2		Bending (100 times)
Kang et al. [43]	Flow & Play	Ag-coated C paper	PDMS	0.98 V	69.1 mW/cm^2		Bending
So et al. [46]	Flow & Play	C cloth	PDMS	0.95V[a]	87.5 mW/cm^2		Bending
Ning et al. [42]	Flow & Play	C paper + CNT membrane	Plastic	0.8 V[a]	145.2 mW/cm^2	10 h (0.6 V)	Bending (600 times)
Ning et al. [44]	Flow & Play	C paper + CNT membrane	PDMS	0.8 V[a]	51.6 mW/cm^2		
Wei et al. [45]	Flow & Play	CNT-coated CNT membrane	PDMS	0.95V[a]	230 mW/cm^2	500 h (50 mA)	Rolling
Novel cell structures							
Hahn et al. [13]	Flow & Play	No GDL	Metal-polymer foil	0.9 V[a]	120 mW/cm^2	23.3 h (80 mW/cm^2)	Bending
Hsu et al. [47]	Flow & Play	C cloth	C fiber + Metal wire	0.9 V[a]	225 mW/cm^2[a]		Bending
Park et al. [48]	Flow & Play	C paper	PC film	1V	89.2 mW/cm^2	120 h (polarization)	Bending (200 times)
Hakola et al. [49]	Flow & Play	C ink	PET	0.68V[a]	0.12 mW/cm^2		
Wang et al. [50]	Inject & Play (formate)	C paper + Au-coated CNT membrane	PDMS	0.86V[a]	82.1 mW/cm^2		Bending

[a] Estimated from the figure of corresponding reference.

bending mode. Table 1 summarizes key features and performances of the reported flexible planar PEMFCs with hydrogen as fuel and air/oxygen as oxidant.

2.1.1. Flexible BPPs

BPP is the outmost layer in a PEMFC single cell, which is responsible for transporting reactant as well as providing assembling pressure. To make it flexible, Wheldon et al. [31] used a polymer material of polyester transparency sheet with no flow channel engraved on it. Instead, the hydrogen and air were blown directly to the electrode surface. Also, the whole device was assembled by a rigid clip to provide sufficient pressure among different layers, which was impractical for real application. Instead of polyester, Chang et al. [32] employed polydimethylsiloxane (PDMS) as BPP with serpentine flow channel for the hydrogen gas, and a metallic film of Ni–Au was sputtered on the surface to improve its electric conductivity. However, when the flexible cell was bended, the power density decreased by 30 % due to the increment of ohmic resistance, which was originated from the cracking of Ni–Au layer during fuel cell bending. To solve this issue, they further deposited an extra layer of Ag nanowire network onto the PDMS BPP as shown in Fig. 3a [33]. This time, the power density was increased from 41 mW/cm^2 at flat status to 71 mW/cm^2 when it was bent (Fig. 3b), which was mainly attributed to the improved compressive force normal to the MEA during bending as shown in Fig. 3c. The well-protected electron conduction path attributed to the extra Ag nanowire was another important reason. In addition, they found that an asymmetric BPP structure with thicker PDMS on the sunken side and thinner one on the extrusion side would further improve the power density to 82 mW/cm^2 [34]. However, this asymmetric design might also impair the cell performance if the bending occurred in the opposite way. Furthermore, the effect of PDMS stiffness on the cell performance was studied, and it was found that a higher BPP stiffness could lead to a higher power output [35]. Meanwhile, this would inversely affect the cell flexibility. Recently, Yoo et al. [38] proposed a pre-bent BPP which exhibited improved power output when external bending was applied. However, its flat-mode performance was lower due to the incomplete contact between the MEA and pre-bent BPP. They also employed 3D printing technique to fabricate the flexible PDMS BPP, which achieved a similar performance at a lower cost of manufacturing [39].

In addition to the BPP material and structure, Park et al. [36] studied the effect of BPP assembling pressure and found that the cell performance would generally increase with its elevation, which was mainly attributed to the decreased ohmic and charge transfer resistance. However, the flow channels inside the PDMS BPP would also be deformed, leading to non-uniform distribution of reactants. They also studied the flexible PEMFC performance under mixed bending and twisting load [37]. It was found that twisting was generally harmful to the cell performance while bending could help to improve the power output. When both deformations occurred, the effect of bending could outperform that of twisting, ensuring a better result than the flat-mode cell. To improve the system integrity, Baek et al. [40] added a 3D-printed PLA frame to contain the flexible PEMFC, with which the cell can be fully folded for 300 times without performance loss. However, this will inevitably increase the cell thickness which is not good for wearable applications. To

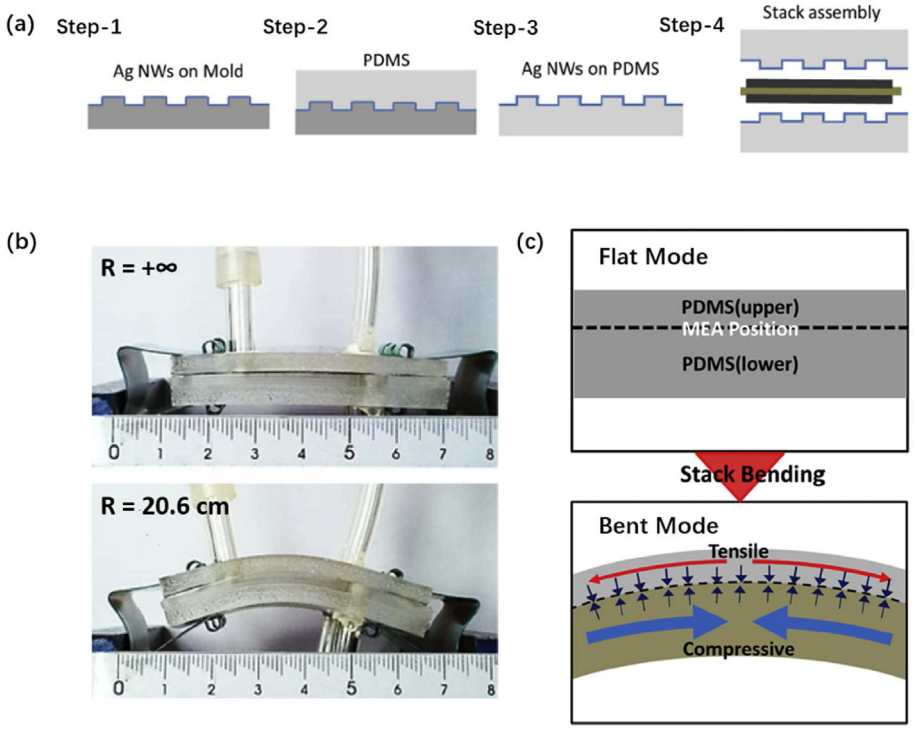

Fig. 3. Flexible BPPs used in PEMFCs: (a) General fabrication process of flexible BPP and PEMFC (Reproduced with permission from Elsevier [34]); (b) Real prototype during bending test (Reproduced with permission from Elsevier [34]); (c) Stress analysis in bent mode (Reproduced with permission from Elsevier [35]).

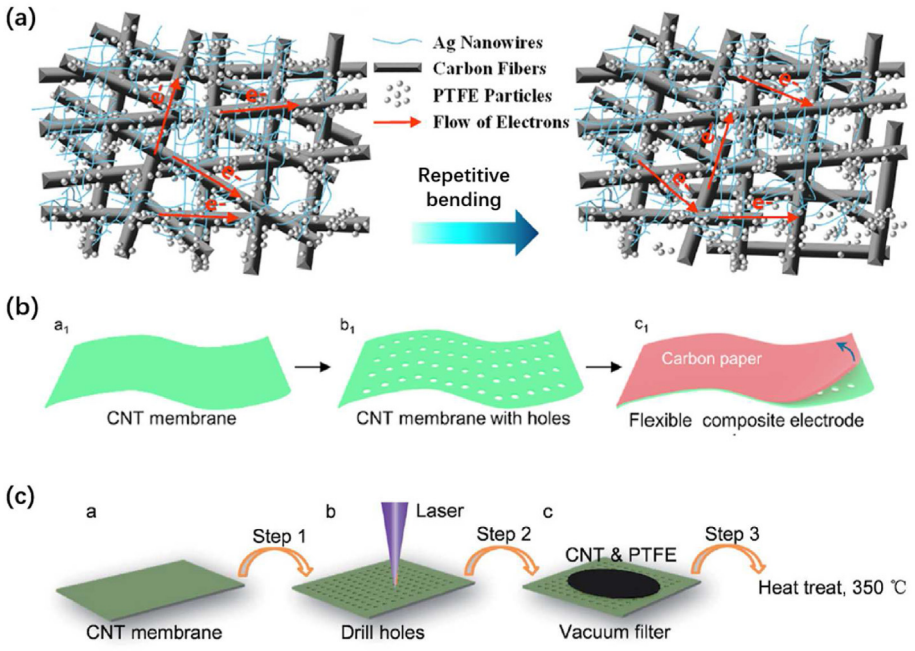

Fig. 4. Flexible GDLs used in PEMFCs: (a) Ag nanowire coated carbon paper (Reproduced with permission from Elsevier [43]); (b) Composite GDL with perforated CNT membrane and carbon paper (Reproduced with permission from ACS [42]); (c) Perforated CNT membrane GDL with extra CNT-PTFE coating (Reproduced with permission from RSC [45]).

sum up, the Ag-coated PDMS BPP is able to ensure a good performance for flexible PEMFC, but its relatively high thickness may hinder the real application on human body, which haven't been studied yet in literature. Also, practical and compact assembling methods other than simple clipping or framing should be investigated in the future.

2.1.2. *Flexible GDLs*

In addition to BPP, GDL is another key to the success of flexible PEMFCs, which is responsible for gas distribution as well as current collection in deformed situations. Kang et al. [41] compared the durability of carbon paper and carbon cloth, two most commonly used

material for GDL, under repetitive bending treatment. They found that the carbon paper-based PEMFC would suffer significant performance loss while the carbon cloth-based one remained robust. This was mainly due to the damage of carbon paper integrity as well as its detachment from the MEA, which induced extra ohmic and charge transfer resistance. They also tried to improve the mechanical integrity of carbon paper for flexible PEMFC considering its higher electric conductivity than carbon cloth [43]. An extra layer of Ag nanowires was coated on the surface of carbon paper, which could connect the broken carbon fibers after repetitive bending, ensuring a stable cell performance (Fig. 4a). So et al. [46] also compared the effect of carbon cloth, carbon paper and carbon cloth with microporous layer during both flat mode and bent mode. It was found that the pristine carbon cloth achieved the highest power density at both modes, which was mainly due to its much lower ohmic resistance.

Instead of using single carbon paper/cloth, Ning et al. [42] developed a composite GDL which was composed of a multi-hole CNT membrane and a carbon paper (Fig. 4b). The multi-hole CNT can provide the necessary flexibility thanks to its excellent mechanical strength, while the carbon paper can better support the electrocatalyst. With this composite GDL, a high power density of 145.2 mW/cm^2 was achievable, and the cell could tolerate 600 times of bending with only 11 % performance loss. In addition to the material aspect, they also studied physical properties of the GDL in flexible PEMFCs [44]. It was found that for a rectangular electrode, the current collection end on the same side of the long edge would lead to the highest power output due to the shortest length of electron transfer pathway. Also, a thicker GDL benefited the cell performance at a price of sacrificed device flexibility. Wei et al. [45] further reduced the GDL thickness by eliminating the usage of carbon paper (Fig. 4c). First, multiple micro pores were created in a CNT membrane by laser, which was next coated by a CNT-PTFE microporous layer. Finally, the 40 μm thick GDL was heat treated at 350 °C and used for MEA development. With this thin-film GDL, the as-fabricated flexible PEMFC could achieve a specific power density as high as 9.7 kW kg^{-1}. The power density was also as high as 230 mW/cm^2, which was 59 % higher than that with carbon paper GDL. In summary, the CNT-based membrane may represent a new type of GDL for flexible PEMFCs, which possesses high mechanical strength and electric conductivity at the same time.

2.1.3. New cell structures

Most of the above-mentioned flexible PEMFCs still require a relatively thick polymer BPP to provide sufficient assembling pressure, which impairs not only the device flexibility but also the energy density. Instead, a thin-film cell structure would be more appropriate for wearable applications. In fact, as early as 2004, Hahn et al. [13] already developed a flexible thin-film PEMFC with a thickness of only 0.2 mm (Fig. 5a), which was targeted for powering microsystems such as wireless sensor networks and chip cards. A metal-polymer composite foil was used as BPP, with the metal foil as substrate and the micro-structured polymer layer as flow channel, while no GDL was used at all to simplify the fabrication process. With hydrogen as fuel, this thin-film PEMFC stack achieved a satisfactory power density of 120 mW/cm^2 with a current output of 40 mA at 1.5 V, which could also discharge at 80 mW/cm^2 for 23.3 h. However, this cell is actually not suitable for wearable applications due to its limited flexibility, especially for the metal part of BPP. Later on, Park et al. [48] developed a rollable PEMFC with a thickness less than 1 mm (Fig. 5b). They employed a 0.2 mm-thick polycarbonate film as BPP, which had flow channels imprinted on it by hot-pressing. To guarantee sufficient assembling pressure, an Au-coated stainless-steel mesh was inserted between the BPP and the MEA as well, which were all assembled by adhesive sealant tape. This thin-film cell exhibited a satisfactory power density of 89.2 mW/cm^2 when bended, which could also function normally when fully rolled into a cylinder-shape. However, the cell performance under flat status was not shown in the paper. Furthermore, Ning et al. [42] and Wei et al. [45] developed thin-film PEMFCs with a thickness of only 0.22 mm and 0.12 mm, respectively, using adhesive to combine the thin BPP and MEA. Nevertheless, with such a thin-film cell structure, the flow channel may be easily distorted or even blocked during practical applications, whose discharge durability needs further investigation especially on the human body.

In addition to the conventional multi-layer structure, other novel cell designs have also been proposed for flexible PEMFCs. To avoid the necessity of assembling pressure, Hsu et al. [47] designed a new current collector based on several bunches of carbon fibers connected by a metal wire (Fig. 5c). The carbon fibers could contact the MEA closely and evenly under bending mode with the help of a wire spring only, ensuring a much-improved power density of 225 mW/cm^2. However, the

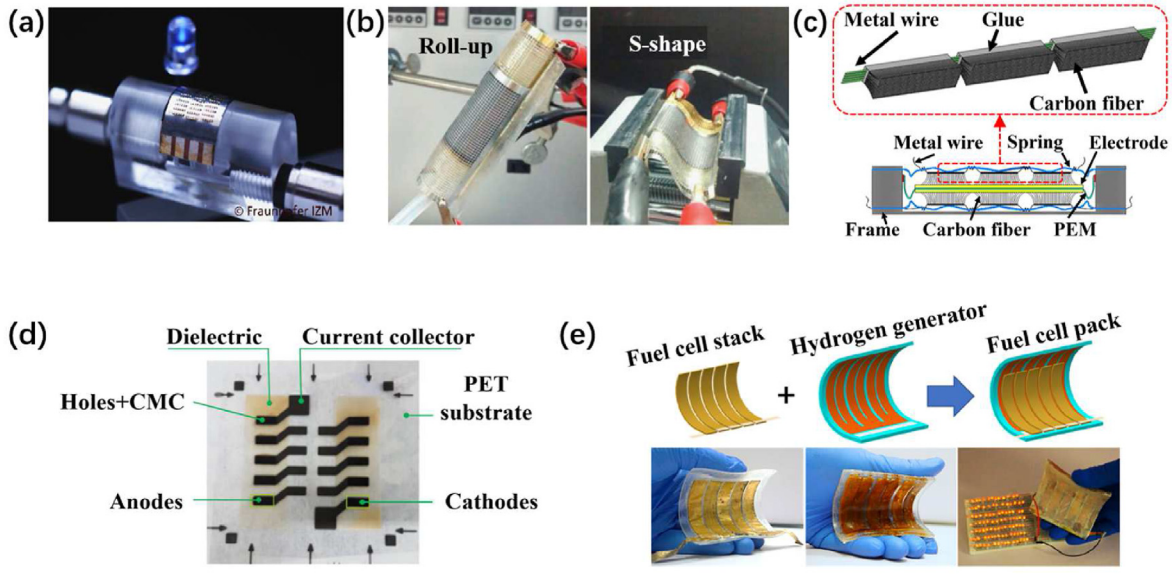

Fig. 5. New cells structures for flexible PEMFC: (a) A thin-film cell based on metal-polymer composite BPP without GDL (Reproduced with permission from Elsevier [13]); (b) A rollable cell based on polymer BPP and metal mesh current collector (Reproduced with permission from Nature [48]); (c) An innovative current collector based on metal wire and carbon fiber (Reproduced with permission from Elsevier [47]); (d) A fully printed cell via screen and inkjet printing (Reproduced with permission from IOP [49]); (e) A flexible hydrogen generator combined with a flexible PEMFC (Reproduced with permission from ACS [50]).

fabrication of this new cell design was quite complicated, and part of the PEM was directly exposed to the ambient air, which might cause water balance problem in real applications. Hakola et al. [49] proposed an innovative inkjet printing method for developing flexible and thin-film PEMFC stack (Fig. 5d). The anode, cathode, polymer electrolyte and current collector were all printed on a PET substrate, while the BPPs with flow channel was fabricated on a PCB base board. However, the power density of this thin-film PEMFC was quite limited, only 0.12 mW/cm^2, even with 50 sccm hydrogen as fuel. This was probably because of the high resistance due to the lack of assembling pressure. Furthermore, most studies tried to make the PEMFC flexible but neglected the flexibility of hydrogen gas storage. To solve this problem, Wang et al. [50] developed a flexible hydrogen generator based on formic acid fuel and an aerogel catalyst, both of which were stored inside a PDMS channel (Fig. 5e). The hydrogen generator could produce 2.4 L hydrogen gas with 4 mL pure formic acid, which was attached to a flexible PEMFC stack and achieved a practical energy density of 135.9 Wh kg^{-1}. However, the formic acid-derived hydrogen may involve CO impurities, which can poison the fuel cell catalyst gradually. To sum up, more long-term durability test should be conducted for flexible PEMFCs with hydrogen fuel, and the flexibility of hydrogen storage and delivery sub-systems also worth further investigation.

2.2. Planar cell design (hydrocarbon fuel)

Considering the high safety need of wearable electronics, liquid hydrocarbon fuels such as methanol, ethanol and formic acid might be more appropriate than hydrogen gas, which also have been explored in literature as summarized in Table 2. However, the power density is much lower than hydrogen due to their sluggish oxidation reaction, which is generally below 20 mW/cm^2.

At first, the acidic Nafion membrane was adopted as electrolyte, and typical direct methanol fuel cell (DMFC) catalysts such as Pt–Ru for anode and Pt for cathode were used. Ito et al. [51] proposed a DMFC stack fabricated on a flexible polysulfone film (Fig. 6a). To simplify the system, methanol fuel was dropped onto the anode surface directly, and a single-cell OCV of 0.56 V and peak power density of 3 mW/cm^2 were successfully demonstrated. Nonetheless, this "Drop & Play" mode is not practical especially for long-term operation. Instead, Weinmueller et al. [52] developed a DMFC with conventional "Flow & Play" mode. An Au-coated SU-8 with multiple pores was used as GDL, while PDMS with microchannels served as BPP. With 1 M methanol solution fed at 0.14 mL min^{-1}, this flexible cell achieved a peak power density of 19 mW/cm^2, but the working temperature was as high as 60 °C. Considering the cumbersome and electricity-consuming pump, a passive feeding mode is more appropriate for wearable fuel cells. Wu et al. [53] developed such a flexible system with methanol fuel provided passively from a fuel tank via capillary action. In addition, since no external assembling components were adopted, the planar cell was rolled into an elliptic cylinder shape in order to utilize the stress from bending. With 30 % methanol solution, this flexible cell output a power density of 15.3 mW/cm^2, which was also demonstrated inside a wrist band to power a LED light. Zhu et al. [54] also developed a passive DMFC stack in which 12 single button cells were integrated in a flexible printed circuit board substrate. A PDMS encapsulation was used to store the methanol solution and distribute it, which could support 67 min of continuous discharge at 12 mA. Alternatively, the methanol fuel can also be prestored inside a hydrogel, so that no external feeding is needed any more. Zou et al. [55] used an agar gel-wood sponge composite material to store methanol fuel, which was next attached to the anode side of a MEA (Fig. 6b). Their flexible cell could be punched, bended, compressed and cut without causing safety issues, and the areal energy density was as high as 13.7 mWh cm^{-2}. Sun et al. [56] also stored methanol fuel in a polyacrylic acid-based gel, and a nanoscale TiC-modified carbon cloth was used as GDL. Benefited from the compact methanol fuel storage, the all-solid flexible DMFC could obtain an energy density as high as 777.8 Wh kg^{-1}. Furthermore, Carneiro et al. [57] employed a paper substrate to store the Nafion polymer and coated the electrode inks directly on the two sides of paper, leading to a monolithic cell structure without GDL and BPP. The methanol fuel was absorbed in paper as well and attached to the anode surface, leading to a power density of 20–50 μW/cm^2. This limited power density could be originated from the poor conductivity of airbrushed electrodes on paper.

To reduce the noble metal loading, alkaline polymer electrolyte based

Table-2
Summary of flexible planar PEMFCs with hydrocarbon fuel.

Reference	Fueling mode	Fuel	GDL	BPP	OCV	Peak Power density	Long-term durability	Flexibility
Nafion membrane electrolyte								
Ito et al. [51]	Drop & Play	Methanol	Au film		0.56V	3 mW/cm^2		Bending (1000 times)
Weinmueller et al. [52]	Flow & Play	Methanol	Au/SU-8	PDMS	0.6V[a]	19 mW/cm^2 (60 °C)		Bending
Wu et al. [53]	Capillary flow	Methanol	C fiber-based film	PDMS	0.6V[a]	15.3 mW/cm^2	21 h (25 mW)	Bending (100 times)
Zhu et al. [54]	Capillary flow	Methanol	XC-72 + PTFE	PMMA	0.5V	7.5 mW/cm^2	67 min (12 mA)	Bending (100 times)
Zou et al. [55]	Prestored in gel	Methanol	CNT film + C paper		0.6V[a]	11 mW/cm^2[a]		Bending; Penetrating; Cutting; Compressing
Sun et al. [56]	Prestored in gel	Methanol	TiC-modified C cloth	PDMS	0.6V[a]	14.1 mW/cm^2	200 min (35 mA/cm^2)	Bending (50 times)
Carneiro et al. [57]	Drop & Play	Methanol	Without	Without	0.45–0.55V	20–50 μW/cm^2		
Hydrogel electrolyte								
Li et al. [58]	Prestored in gel	Methanol	Unknown		0.5V	8.9 mW/cm^2	54 h (0.5 mA/cm^2)	Bending
Wang et al. [59]	Drop & Play	Ethanol	C cloth		0.73V	21.5 mW/cm^2	21 h (0.1 mA/cm^2)	Bending (1000 times)
Jiang et al. [60]	Drop & Play	Ethanol	C cloth		0.66V	9.2 mW/cm^2	8 h (0.1 mA/cm^2)	Bending (1200 times)
Li et al. [61]	Drop & Play	Ethanol	C cloth		0.6V	12.7 mW/cm^2	120 h (0.25 mA/cm^2)	Bending (700 times)
Yang et al. [62]	Prestored in gel	Formic acid	C cloth		0.75V	2.83 mW/cm^2		Bending; Twisting; Needling

[a] Estimated from the figure of corresponding reference.

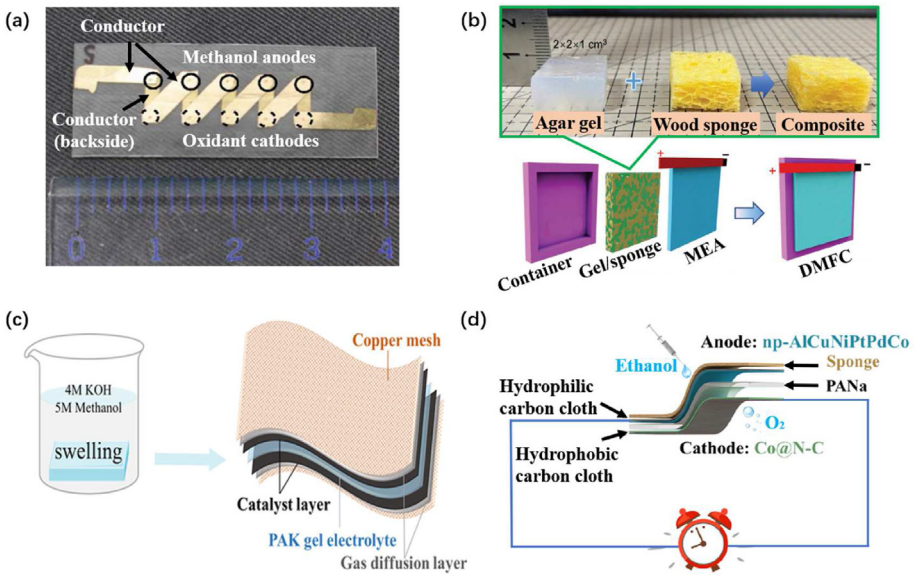

Fig. 6. Flexible PEMFCs with hydrocarbon fuel: (a) Nafion-based cell with "Drop & Play mode" (Reproduced with permission from Elsevier [51]); (b) Nafion-based cell with fuel prestored in gel (Reproduced with permission from Wiley [55]); (c) Alkaline gel-based cell with fuel prestored in gel electrolyte (Reproduced with permission from ACS [58]); (d) Alkaline gel-based cell with "Drop & Play mode" (Reproduced with permission from Elsevier [60]).

on hydrogel was also studied instead of Nafion membrane, enabling the utilization of various non-noble catalysts. Li et al. [58] prepared a kalium polyacrylate hydrogel saturated with KOH solution and methanol fuel as the polymer electrolyte, so that a Fe single-atom catalyst could be used for the cathode (Fig. 6c). A peak power density of 8.9 mW/cm^2 was achieved, and the cell could discharge continuously for 54 h with the prestored methanol in gel. However, since methanol is toxic to the human body, the ethanol fuel would be a much safer choice despite its slower reaction kinetics. Wang et al. [59] employed the sodium polyacrylate (PANa) to hold KOH solution, which was 100 % stretchable without losing its ionic conductivity. With an ethanol-tolerant N, S-doped carbon catalyst for the cathode, the ethanol fuel can be dropped directly to the anode side without fuel crossover side effect. The peak power density was as high as 21.5 mW/cm^2, and the cell could tolerate 1000 times of bending with 68 % of initial performance reserved. Instead of using Pt–Ru as anode catalyst, Jiang et al. [60] prepared an Al–Ni–Cu–Pt–Pd–Co senary catalyst via a dealloying method, and the PANa-KOH hydrogel was used as polymer electrolyte as well (Fig. 6d). When 1 mL ethanol was provided, the power density of 9.2 mW/cm^2 was lower, but the device cost could be further reduced due to the deceasing of noble metal loading. The same group also proposed an Al–Pd–Ni–Cu–Mo anode catalyst for the gel-electrolyte ethanol fuel cell, which improved the peak power density to 12.7 mW/cm^2 [61]. More importantly, the areal energy density was significantly improved to 13.6 mWh cm^{-2}, and the cell could be discharged at 0.25 mA cm^{-2} for almost 120 h. Despite the improved reaction kinetics, alkaline polymer electrolytes would be gradually carbonated by CO_2 in the ambient air, so that the fuel cell lifetime needs to be further investigated. Instead of alkaline hydrogel, Yang et al. [62] developed an acid hydrogel based on H_2SO_4 and polyvinyl alcohol-polyvinyl pyrrolidone-sulfosuccinic acid, which also contained formic acid fuel inside. A limited power density of 2.83 mW/cm^2 was achieved which was probably due to the mediocre ORR catalyst (activated carbon), but the cell could work normally after bending, twisting and needling.

2.3. Tubular cell design

Unlike the planar PEMFC whose cell components are stacked one on top of the other, the tubular PEMFC generally adopts coaxial cell components which are wrapped from inside to outside. Considering the fuel delivery and air-breathing needs, the anode tube is generally placed inside so that the fuel flow channel is naturally formed, while the cathode tube is placed outside to freely breathe the ambient air. In the middle, a polymer electrolyte tube is used to separate the two electrodes. Such a cell design has several advantages, including easy sealing, inherent assembling pressure and alleviated cathodic overpotential loss. In addition, when it comes to wearable applications, the tubular cell with small diameter can be seamed into clothes, or be fully woven into a fuel cell textile to provide higher power output. Nevertheless, the fabrication of tubular PEMFCs so far is more complex, and the modularity is lower than its planar counterpart. Therefore, relevant research works are very scarce in literature. Eickhoff [63] developed a tubular flexible PEMFC using a porous lithium aluminum hydride as the solid core, while the hydrogen anode, PEM and air cathode were wrapped on its surface sequentially (Fig. 7a). The lithium aluminum hydride could react with water either from the fuel cell reaction or from the ambient environment and generate hydrogen for the anode reaction. Therefore, this fuel cell was more like a battery without continuous operation ability. Alternatively, Yang et al. [64] used formic acid diluted solution as fuel. Their tubular cell had a solid anode fiber in the center, which was surrounded by a cation exchange membrane as separator and an external layer of cathode based on carbon cloth (Fig. 7b). When the formic acid solution was injected into the fuel cell tube, a limited power density of 0.46 mW/cm^2 was obtained, which was probably due to the low fuel concentration as well as the sluggish oxygen transport. Instead of developing long fuel cell tubes monolithically, Hwang et al. [65] recently proposed a short conical cell design which could be connected into long fuel cell stack in the manner of overlapping paper cups without the need of extra assembling components (Fig. 7c). A reverse truss origami design was also proposed for connecting the single cells in order to improve the device flexibility. With hydrogen as fuel, their tubular cell could output a power density of 111 mW/cm^2, which was comparative to planar cells. When using methanol fuel instead, the power density was decreased to 3.8 mW/cm^2. In summary, the development of tubular flexible PEMFCs is still in a very early stage, while more efforts should be paid to their structure, system and durability study.

3. Flexible MFCs

At the moment, commercial PEM such as Nafion® is still quite

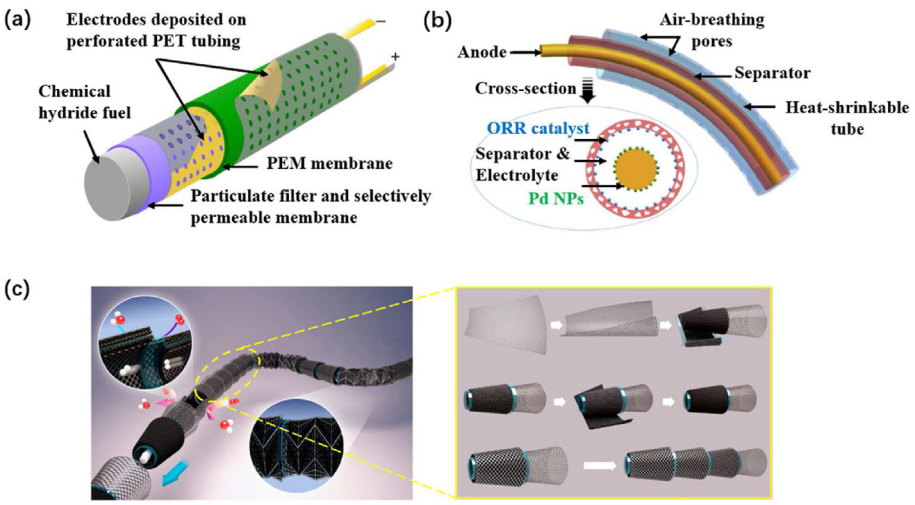

Fig. 7. Tubular flexible PEMFCs reported in literature: (a) A hydrogen cell with all its components wrapped on a lithium aluminum hydride core which provides hydrogen (Reproduced with permission from SPIE [63]); (b) A formic acid cell with all its components sealed in a heat shrinkable tube which is injected with fuel solution (Reproduced with permission from Elsevier [64]); (c) An overlapping paper cups-like stack with conical-shape single cells (Reproduced with permission from ACS [65]).

expensive, which also has delicate requirement on the water management in order to maintain a high ionic conductivity yet avoid the flooding problem. Considering this, the membraneless fuel cell (MFC), also known as microfluidic fuel cell, has been proposed, which adopts microfluidic flows between the two electrodes instead of PEM [15]. Typically, two flows are employed with fuel dissolved in one (the anolyte) and oxidant in the other (the catholyte), which can co-exist in the confined channel without vigorous mixing due to the low Reynolds number. Specifically, when the oxidant is from ambient air and the cathode catalyst is fuel-tolerant, only one anolyte flow is needed, leading to improved system simplicity as well as operation stability. This type of low-cost fuel cell is very competitive for wearable applications, which can be divided into three sub-types based on their substrate material. The plastic-based MFC generally engraves its microfluidic channel in a thin-film plastic chip, with all other cell components integrated on it as well. The paper-based MFC generally deposits its electrodes on a single piece of cellulose paper, while the liquid electrolyte is transported inside by capillary action only. As for the thread-based MFC, a cotton thread is adopted as substrate to obtain a tubular cell structure, which shares a similar working mechanism with the paper-based type. The following sections will introduce them separately.

3.1. Plastic-based MFCs

The first batch of MFCs were fabricated on plastic substrates such as polymethyl methacrylate (PMMA) and polydimethylsiloxane (PDMS). To make them flexible, thickness of the plastic substrate should be reduced significantly. As shown in Fig. 8, Tominaka et al. [66] first developed a

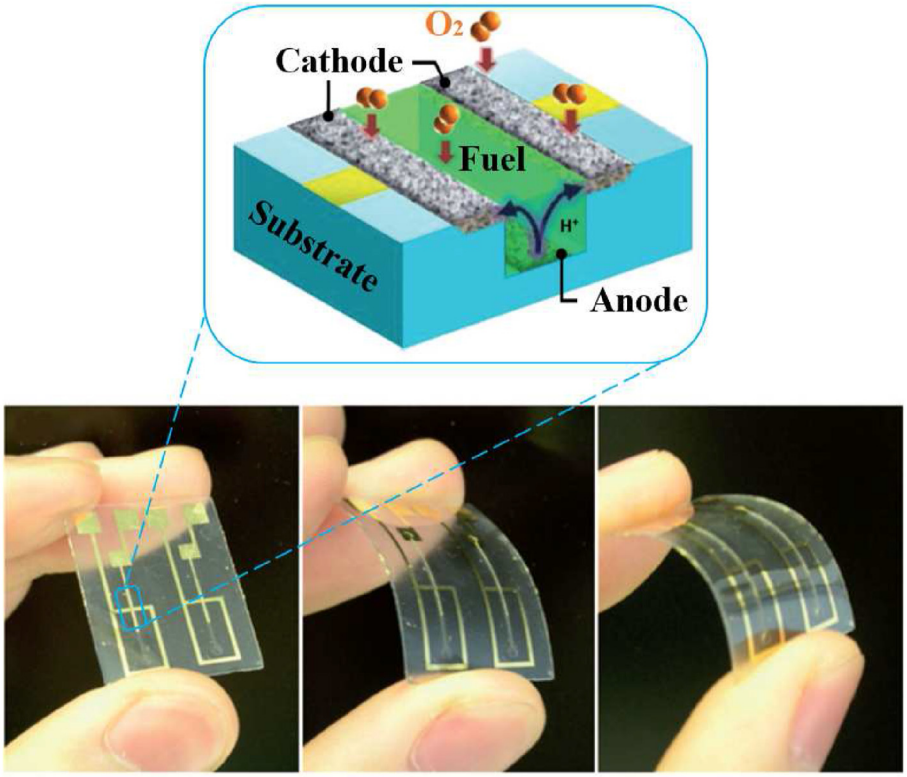

Fig. 8. A typical plastic-based flexible MFC (Reproduced with permission from RSC [66]).

bendable on-chip fuel cell on a flexible cycloolefin polymer film. The methanol fuel and acid electrolyte solution were delivered through the microchannel via capillary action without active pumping, leading to a power density of 0.08 mW/cm^2. However, the cell flexibility during operation was not demonstrated. Ortiz-Ortega et al. [67] employed polyester foil and silicone elastomer film as substrate, together with carbon nanofoam-based flow-through electrodes. An impressive peak power density of 132 mW/cm^2 was achieved using formic acid as fuel, probably due to the improved electrochemical surface area, and the cell could also be bended for 30°. Nevertheless, an active pumping was necessary to ensure the discharge stability, which inevitably impair flexibility of the whole system. Recently, Yang et al. [68] designed a direct H_2O_2 membraneless fuel cell using Ni foam as anode, Prussian blue and reduced graphene oxide on carbon cloth as cathode, and a PMMA thin layer in between as the microfluidic channel. The fuel and electrolyte solution were injected onto the porous anode to start the reaction, leading to a power output of 0.22 mW/cm^2, and a bending angle of 45° was successfully demonstrated. Still, a pump was needed for continuous

Table-3
Summary of paper-based MFCs reported in literature.

Reference	Anode	Fuel	Electrolyte	Oxidant	Cathode	OCV	Power density	Durability
Dual-flow cells								
Esquivel et al. [72]	Pt–Ru/C	Methanol	KOH	Air	Pt/C	0.52 V	4.4 mW/cm^2	7 min (10 mA/cm^2)
Arun et al. [73]	Pencil stroked graphite	Formic acid	H_2SO_4	Air	Pencil stroked graphite	0.33 V	32 mW/cm^2	1000 min (OCV)
Rao et al. [74]	Pencil stroked graphite	Formic acid	H_2SO_4	Air	Pencil stroked graphite	0.33 V	0.07 mW/cm^2	220 min (OCV)
Rao et al. [75]	Pencil stroked graphite	Formic acid	H_2SO_4	Air	Pencil stroked graphite	0.46 V	0.17 mW/cm^2	110 min (0.18 mA/cm^2)
Lal et al. [76]	Graphite sheet	Formic acid	H_2SO_4	$KMnO_4$	Graphite sheet	1.3V	0.57 mW/cm^2	
Copenhaver et al. [77]	Pd/C	Formate	KOH–KCl	H_2O_2	Colloidal graphite	0.7 V[a]	12.5 mW/cm^2[a]	70 min (1 mA/cm^2)
Galvan et al. [78]	Pd/C	Formate		H_2O_2	Activated carbon	1.1 V	2.5 mW/cm^2	
Ma et al. [79]	Pd/C	Formate	H_2SO_4– KOH	H_2O_2	Pd/C	1.5 V	10.8 mW/cm^2	
Li et al. [80]	Pt/C	Formate	KOH–KCl	H_2O_2	Pt/C	0.99 V	7.3 mW/cm^2	
Liu et al. [81]	Pd	Formate	H_2SO_4– KOH	H_2O_2	Pd	1.42 V	12.9 mW/cm^2	
Purohit et al. [82]	Pd/C	Formate		$AgNO_3$	Carbon	1.1 V	4.1 mW/cm^2	100 min (2 mA/cm^2)
Shen et al. [83]	Pd/C	Formate	KOH	Air	Pd/C	0.86 V	7.1 mW/cm^2	60 min (0.4 V)
Wang et al. [84]	Pd foam	Formate	KOH	Air	Pd foam	0.8 V	2.1 mW/cm^2	
Chandra et al. [85]	MoO_3 nanorods	Ethanol	H_2SO_4	$K_2Cr_2O_7$	MoO_3 nanorods	1.4 V[a]	6.3 mW/cm^2	
Lima et al. [86]	Pt/C	Ethylene glycol	H_2SO_4–KOH	$Na_2S_2O_8$	Carbon	0.38 V	6.8 mW/cm^2	
Pasala et al. [87]	Ni mesh	$NaBH_4$	H_2SO_4–NaOH	VO_2^+	C paper	2.1 V[a]	4.5 mW/cm^2	100 min (1 V)
Jung et al. [88]	Graphene	V^{2+}	H_2SO_4	VO_2^+	Graphene	1.15 V	15.1 mW/cm^2	26.7 min (at 10 mA/cm^2)
Chino et al. [89]	Pt	Urea	KOH	$AgNO_3$	Graphite	0.6 V	0.91 mW/cm^2	60 min (0.25 mA/cm^2)
Luo et al. [90]	Ni foam	H_2O_2	HCl–KOH	H_2O_2	Prussian blue/CNT	1 V	10.2 mW/cm^2	28 h (1 mA/cm^2)
Verma et al. [91]	Au/NiO	$Na_2CO_3{\cdot}1.5H_2O_2$	H_2SO_4–NaOH	$KMnO_4$	Au/NiO	1.25V[a]	2.6 mW/cm^2	10–20 min
Lal et al. [92]	Cu-NPs@f-MWCNTs	$N_2H_4{\cdot}H_2O$	H_2SO_4–NaOH	$KMnO_4$	f-MWCNTs	1.8V	3.57 mW/cm^2	10min (1 μA)
Single-flow cells								
Ehteshami et al. [93]	Al	H_2O_2	HCl	H_2O_2	Prussian blue	0.61 V	0.81 mW/cm^2	50 min (0.3 V)
Yan et al. [94]	Ag nanowire	H_2O_2	H_2SO_4	H_2O_2	Prussian blue/CNT	0.58 V	0.88 mW/cm^2	3 min (4 mA/cm^2)
Arun et al. [95]	Pencil stroked graphite	Formic acid	H_2SO_4	Air	Pencil stroked graphite	0.36 V	4 mW/cm^2	60 min (OCV)
Luo et al. [96]	Pd/C	Formate	KOH	Air	MnO_2/CNT	0.94 V	20 mW/cm^2	270 h (at 5 mA/cm^2)
Esquivel et al. [97]	Pt	H_2	KOH	Air	Pt	0.9 V	103 mW/cm^2	60 min (20 Ω)
Wang et al. [98]	Pt/C	H_2	NaOH	Air	MnO_2/CNT	0.93 V	4 mW/cm^2	333 min (1 mA/cm^2)
Ji et al. [99]	Vit B_{12} || Bucky paper	Vitamin C	PBS	Dissolved O_2	BOD || Bucky paper	0.45V	0.17 mW/cm^2	12 h
Paper-like substrates								
Asadnia et al. [100]	Al	H_2O_2	HCl	H_2O_2	Prussian blue	0.65 V	1 mW/cm^2	
Park et al. [101]	Al	H_2O_2	HCl	H_2O_2	Prussian blue	0.98 V	1.43 mW/cm^2	618 min (0.9 mA/cm^2)
Domalaon et al. [102]	Pd/C	Formate		H_2O_2	Activated carbon	0.92 V	4.4 mW/cm^2	
Liu et al. [103]	Pd	Formate	H_2SO_4–KOH	H_2O_2	Pd	1.35 V	8.9 mW/cm^2	3000 s (at 0.6 V)
Zhai et al. [104]	Au nanowire	Ethanol	NaOH	Air	Pt/Au nanowire	0.4V	0.08 mW/cm^2	
Gong et al. [105]	Au nanowire || polyHIPEs	Ethanol	KOH	Air	Pt/Au nanowire || polyHIPEs	0.33 V[a]	0.28 mW/cm^2	
Lu et al. [106]	Au–Pd nanowire	Ethanol	KOH	Dissolved air	Au nanowire	0.49 V	0.49 mW/cm^2	500 stretch cycles

[a] Estimated from the figure of corresponding reference.

operation. In summary, the necessity of an active pump may be the major obstacle for chip-based MFCs, and the associated tubing and connection can also impair the system flexibility.

3.2. Paper-based MFCs

Compared with plastic chip, cellulose paper is a natural material with inherent high flexibility, which has already been widely adopted as substrate for metal ion batteries, metal-air batteries, supercapacitors, solar cells, nanogenerators, and so on [69–71]. As for the fuel cell, the paper substrate has an extra advantage of pumpless operation thanks to its capillary action, which can greatly simplify the energy system. Table-3 summarizes different types of paper-based fuel cells reported in literature. Based on the number of electrolyte inputs, they can be classified into the dual-flow and the single-flow type. The former case follows the conventional MFC design with classic Y-shape channel, which adopts anolyte for fuel and catholyte for oxidant delivery. The latter case employs only one flow of electrolyte with no need for separation thanks to the fuel-tolerant cathodic catalyst, which is more convenient for practical applications. Moreover, some paper-like materials such as cotton and sponge were also included in this section.

Fig. 9a exhibits the typical structure for a dual-flow paper-based MFC. In 2014, Esquivel et al. [72] and Arun et al. [73] first proposed the concept of paper-based MFC with the Y-shape paper channel, using methanol and formic acid as fuel, respectively. The methanol oxidation reaction is relatively sluggish which also requires high-cost Pt–Ru as catalyst, providing a peak power density of 4.4 mW/cm^2. On the contrary, the formic acid fuel was oxidized efficiently by pencil-stroked graphite only, and a relatively high power density of 32 mW/cm^2 was reported. Rao et al. also employed the pencil-stroked graphite as electrodes for the formic acid fuel, but the power output was much smaller in their studies, only 0.07 [74] and 0.17 mW/cm^2 [75], respectively, indicating that the property of pencil-stroked graphite needs deeper investigation. Lal et al. [76] tried another carbon material of graphite sheet for the formic acid fuel, and the power density of 0.57 mW/cm^2 was also quite limited. Compared with the volatile and pungent formic acid fuel, the formate salt may be a better choice, whose alkaline reaction environment also allows the utilization of non-noble metal catalysts [77–84]. For the anode side, palladium catalyst is requisite for the efficient oxidation of formate, while various oxidants such as H_2O_2 [77–81], $AgNO_3$ [82] and air [83,84] were employed for the cathode side. The OCV could reach as high as 1.1 V, while the peak power output was generally below 10 mW/cm^2. Shen et al. [83] investigated the effect of paper structure and found that larger pore diameter led to higher OCV and power density, which was due to the minimized fuel depletion. Li et al. [80] developed a vertical paper-based MFC stack and found that the overlapped filter paper could enhance the capillary flow and therefore greatly improve the stack performance. Wang et al. [84] employed simulated sunlight to affect the water evaporation rate of the absorption pad, so that the electrolyte capillary flow rate could be controlled precisely. However, this would inevitably complex the whole energy system. Ma et al. [79] studied the effect of ambient temperature and humidity on the cell performance. It was found that the ambient temperature had a significant influence on the cell activation and power output, while the effect of ambient humidity was not obvious. To reduce the Pd loading, Liu et al. [81] proposed a stepped catalyst layer design in which the Pd catalyst was reduced in the downstream part of electrode. This would not decrease the cell performance because of the fuel depletion effect along the electrode length. In addition to these common fuels, other choices such as ethanol [85], ethylene glycol [86], sodium borohydride [87], vanadium species [88], urea [89], hydrogen peroxide [90,91] and hydrazine [92] were also tried in the dual-flow paper-based MFC, and the power density were generally below 10 mW/cm^2.

Compared with the dual-flow design, the single-flow paper-based MFC is more practical for wearable applications, which requires only one electrolyte input as shown in Fig. 9b. To achieve this, H_2O_2 is a suitable reactant which can function as both fuel and oxidant thanks to its intermediate valence of oxygen. Ehteshami et al. [93] developed a paper-based H_2O_2 MFC by using aluminum and Prussian blue as selective catalyst for the anode and cathode, respectively. An OCV of 0.61 V and a peak power density of 0.81 mW/cm^2 were obtained even when the cell was bended or distorted. However, the aluminum anode was also consumed during fuel cell operation, which would impair the device durability. Instead of aluminum, Yan et al. [94] used silver nanowire as the anode catalyst for H_2O_2 oxidation. The OCV of 0.58 V and peak power density of 0.88 mW/cm^2 was similar to the previous work, while long-term durability result was not provided. In addition to H_2O_2, if a fuel-tolerant ORR catalyst is adopted for catalyzing the ambient air,

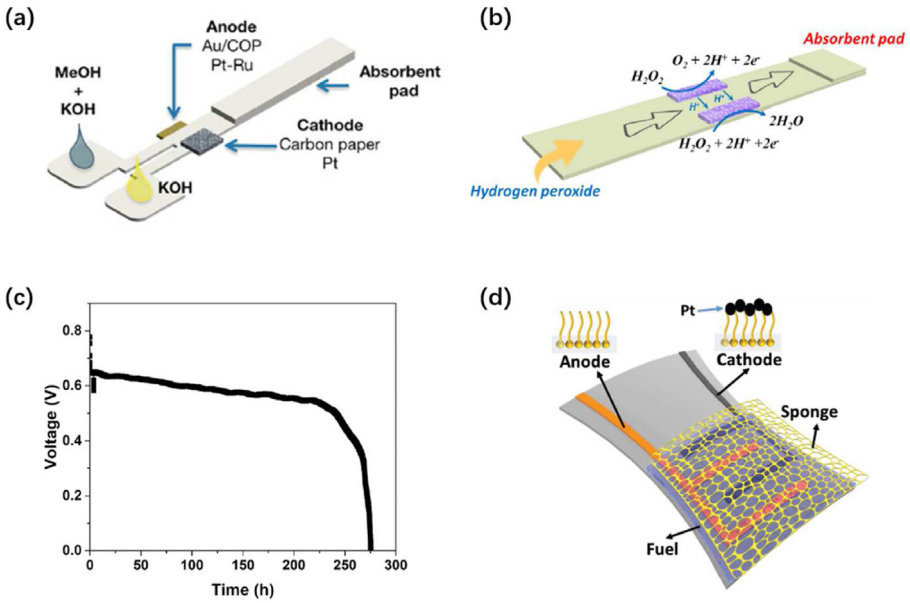

Fig. 9. Paper-based flexible MFCs: (a) The dual-flow cell design (Reproduced with permission from RSC [72]); (b) The single-flow cell design (Reproduced with permission from Wiley [94]); (c) Long-term discharge test of a paper-based formate MFC (Reproduced with permission from Elsevier [96]); (d) Flexible MFCs with paper-like substrates such as sponge (Reproduced with permission from Wiley [104]).

conventional fuels such as formic acid and formate can also be used without fuel crossover side effect. Arun et al. [95] used the pencil-stroked graphite as cathode catalyst so that only a single flow of formic acid and sulfuric acid solution was provided, leading to an OCV of 0.36 V and a power density of 4 mW/cm^2. However, the long-term durability was not studied in their work. Luo et al. [96] employed manganese dioxide as the fuel-tolerant cathode catalyst, and the whole anode was immersed in a cartridge storing the formate and alkaline solution. In this manner, both the ionic conductivity and fuel supply rate were enhanced, leading to an improved power density of 20 mW/cm^2. The fuel cell was discharged stably at 5 mA cm^{-2} for more than 10 days as shown in Fig. 9c, which was also recoverable after refueling, proving the high durability of paper-based MFCs. Furthermore, the hydrogen fuel can be used and only one flow of electrolyte solution is needed to separate it from the ambient air. To eliminate the need for hydrogen storage, Esquivel et al. [97] stored Mg–Fe alloy inside their fuel cell device, which can react with electrolyte to generate hydrogen fuel in-situ. A superior power density of 103.2 mW/cm^2 was demonstrated, which was even comparable with the flexible PEMFCs. Nevertheless, the whole device had a poor flexibility due to the need for Mg–Fe storage, hydrogen chamber and plastic shell. Instead, Wang et al. [98] employed a thin aluminum foil as hydrogen source and embedded it into the paper substrate. With printed anode and cathode inks, the whole fuel cell had a similar thickness with a single piece of paper, which could be bended for 135° without performance loss. However, the power density of 4 mW/cm^2 was lower due to the mild hydrogen generation reaction. Other fuels such as vitamin C [99] was less studied in literature.

In spite of the inherent flexibility of paper substrate, most paper-based MFCs in literature still require an extra plastic shell to support the cell components, so that the whole device flexibility was significantly impaired. From the practical point of view, the single-flow cell design with a replaceable anolyte cartridge is more appealing, which was already proved to be operated for hundreds of hours stably. Nevertheless, the natural cellulose fiber is still not robust enough when encountering competitive deformations in wet mode especially for stretching, which tends to be torn part gradually. Therefore, other paper-like fibrous materials with enhanced physical and chemical robustness have also been explored, such as the electrospun PVDF nanofiber [100], cotton [101, 102], carbon cloth [103], PDMS [106] and sponge [104] (Fig. 9d). Furthermore, the substrate can be fully eliminated by depositing electrodes on the skin directly, which obtain fuel and electrolyte from sweat [105]. In fact, this strategy is more popular with BFCs as will be introduced in Section-4.

3.3. Thread-based MFCs

The flexible MFC can also be fabricated in a tubular manner by using cotton thread as substrate, which also delivers electrolyte via the capillary action. Table 4 summarizes thread-based MFCs reported in recent literature, including the dual-flow formate cell and the single-flow H_2O_2 cell.

Liu et al. [107] first proposed the thread-based MFC using formate as fuel and H_2O_2 as oxidant. Two cotton threads were wrapped onto two Pd-loaded graphite rods, which were next placed in parallel and served as the anode and cathode, respectively. In between, a third thread was used as a separator. However, this cell was actually not flexible due to the rigid graphite electrodes. Instead of graphite rod, Wu et al. [108] used carbon paper to support the catalyst, which was placed beneath the cotton thread channel. Dissolved oxygen in electrolyte was used as oxidant instead of H_2O_2, leading to a power density of 19.9 mW/cm^2. This design still required a glass plate to support all the cell components. To remove the necessity of any external electrodes, Wang et al. [109] dipped cotton thread into a Pd-CNT ink for multiple times, so that a flexible and flow-through electrode was obtained as shown in Fig. 10a. Benefited from the enlarged reaction surface area, the peak power density was increased to 24.8 mW/cm^2. However, since the cotton thread itself is a non-conductive material, an extra carbon paper was still needed as the current collector. To better solve this flexibility issue, new fiber material was proposed for the electrode part instead of cotton thread by Liu et al. [110]. They braided conductive carbon fibers into a 3D herringbone-like pattern and deposited the Pd catalyst onto its electrode part, which was used for both electrochemical reaction and electrolyte delivery. This new cell design achieved the highest power density of 29.9 mW/cm^2 so far among all its kinds, but it is still one step away from wearable applications due to the rigid packaging. To solve this problem, they stored the braided anode inside a silicon rubber tube and fixed the carbon cloth-based cathode on the outer surface, while only one electrolyte of formate and KOH was flowed in the tube [111]. In this manner, a highly flexible version of single-flow formate MFC was achieved, which could keep 90.9 % power density after 1000 bending times.

To simplify the system, H_2O_2 serving as both fuel and oxidant enables a single-flow configuration for the thread-based MFC. Liu et al. [112] studied this by using Ni mesh as anode and Prussian Blue on carbon cloth as cathode, which were both placed beneath the cotton thread channel (Fig. 10b). A mixed solution of H_2O_2–HCl was supplied continuously via the cotton thread, leading to a moderate peak power density of 5.5 mW/cm^2. However, their cell still involved rigid supporting and covering

Table-4
Summary of thread-based MFCs reported in literature.

Reference	Anode	Fuel	Electrolyte	Oxidant	Cathode	OCV	Power density	Durability	Flexibility
Liu et al. [107]	Pd || graphite rod	Formate	H_2SO_4–KOH	H_2O_2	Pd || graphite rod	1.44 V	20.7 mW/cm^2	60 min (at OCV)	
Wu et al. [108]	Pd ||C paper	Formate	KOH	Dissolved O_2	Pt ||C paper	0.91 V	19.9 mW/cm^2	60 min (at 0.35 V)	
Wang et al. [109]	Pd-CNT || cotton thread	Formate	Na_2SO_4	H_2O_2	Pd-CNT || cotton thread	1.41 V	24.8 mW/cm^2	300 min (at 0.63 V)	
Liu et al. [110]	Pd ||C fiber	Formate	H_2SO_4–KOH	H_2O_2	Pd ||C fiber	1.44 V	29.9 mW/cm^2	50 min (at 0.8 V)	
Liu et al. [111]	Pd ||C fiber	Formate	KOH	Air-breathing	Co@NPC/C-MWCNTs ||C cloth	1 V*	4.32 mW/cm^2	50 min (at 0.33 V)	Bending (1000 times)
Liu et al. [112]	Ni mesh	H_2O_2	HCl	H_2O_2	PB/CNT ||C cloth	0.66 V	5.5 mW/cm^2	1000s (at 0.3 V)	
Zhou et al. [113]	Ni || CNT yarn	H_2O_2	$HClO_4$ + NaCl	H_2O_2	$Fe_3[Co(CN)_6]_2$ || CNT yarn	0.88 V	6.3 mW/cm^2	11.6 days (at OCV)	Bending (350 times)
Wang et al. [114]	Ni ||C fiber	H_2O_2	HCl	H_2O_2	PB-MWCNT ||C fiber	0.65 V	14.4 mW/cm^2	40 min (at 0.29 V)	Bending (10 times)

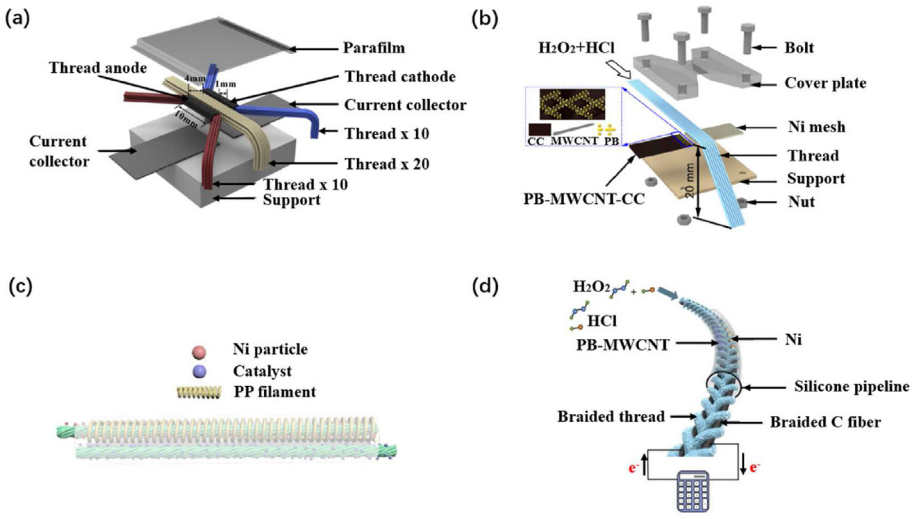

Fig. 10. Thread-based flexible MFCs: (a) Dual-flow formate cell with three electrolyte inputs and supporting plate (Reproduced with permission from Elsevier [109]); (b) Single-flow H_2O_2 cell with only one electrolyte input and supporting plate (Reproduced with permission from ACS [112]); (c) Single-flow H_2O_2 cell with a tubular structure based on bi-scrolled CNT yarn (Reproduced with permission from Wiley [113]); (d) Single-flow H_2O_2 cell with a tubular structure based on braided carbon fiber (Reproduced with permission from Elsevier [114]).

plates. To make it fully flexible, Zhou et al. [113] proposed a tubular MFC based on bi-scrolled CNT yarn. Both anode and cathode catalysts were deposited onto corresponding CNT yarns, which were next encapsuled in a silicon tube as shown in Fig. 10c. To prevent short-circuiting, an extra polypropylene filament was wrapped onto the anode yarn. When the fuel and electrolyte solution was injected into the tube, a power density of 6.3 mW/cm^2 was obtained, and the cell could be bended for more than 350 cycles without performance loss. Recently, Wang et al. [114] also developed an advanced tubular cell using braided carbon fiber as electrode and cotton thread as separator (Fig. 10d). First, catalysts were deposited onto the carbon fiber to form the flow-through anode/cathode, and the cotton thread was knitted into a flow channel. Next, the anode and cathode were inserted into the flow channel separately without contacting each other. Finally, the whole device was sealed in a silicon pipeline. When H_2O_2–HCl mixed solution was wicked by the cotton thread, an enhanced power output of 14.4 mW/cm^2 was exhibited, and the device could tolerate a bending degree of 60° for 10 times. To sum up, the thread-based MFC is more suitable to be encapsuled in a tube rather than on a plate, which can next be sewed into clothes for powering wearable applications.

4. Flexible BFCs

In addition to the above-mentioned abiotic catalysts such as noble metals, metal oxides and carbonaceous materials, bio-catalysts including enzymes and microbes can also be used in fuel cell electrodes, which has many distinct advantages such as low cost, high renewability and mild operation environment. Correspondingly, the obtained biofuel cells (BFC), including enzymatic fuel cells and microbial fuel cells, are especially suitable for wearable applications in terms of cost and safety. Their flexible version is also under extensive research in recent years.

4.1. Enzymatic fuel cells

Enzyme is a kind of protein or RNA which can catalyze bioreactions selectively and efficiently even in a mild environment. By adopting enzyme as biocatalysts, the enzymatic fuel cell can consume various biofuels such as glucose, lactate and fructose from the human body, so that it is very promising for powering wearable electronics without external fuel supply. Table 5 summarizes flexible enzymatic fuel cells reported to date, which generally deliver a peak power density from several μW cm^{-2} to even several mW cm^{-2}. Different cell substrates have been explored to date as shown in Fig. 11, including contact lenses-based cells, tattoo-based epidermal cells, textile-based cells, paper-based cells and gel-electrolyte cells. The former four cases tend to obtain fuel directly from the body fluid such as tear and sweat, which contains sufficient glucose/lactate fuel. The gel-electrolyte cells choose to pre-store fuel inside the gel, so that they function more like the conventional battery with limited lifetime. Furthermore, flexible enzymatic fuel cells based on polymer films have also been reported as shown in Fig. 11f, but the power density was quite limited at the moment (~1 μW/cm^2) [115–117].

4.1.1. Contact lenses-based cells

The first batch of wearable enzymatic fuel cells were developed based on contact lenses, which were designed to harvest energy from the human tear. Falk et al. [118] used Au wires coated with Au nanoparticles as electrodes to support the cellobiose dehydrogenase and bilirubin oxidase (Fig. 11a), which could catalyze the glucose oxidation and oxygen reduction from the tear, respectively. A OCV of 0.57 V and a power density of 1 μW/cm^2 were demonstrated, which also showed an operational half-life of more than 20 h. Instead of glucose, they also tried to utilize the ascorbate in tear as fuel, which could be oxidized by a conducting complex in anode [119]. The power density was improved to 3.1 μW/cm^2, and the fuel cell could also be coupled with a glucose biosensor for continuous health monitoring of diabetes patients. Xiao et al. [120] chose lactate in tear as fuel, and an electrochemical dealloying method was used to prepare the nano-porous Au electrodes on contact lenses. When tested by synthetic tear solution, the power density of 1.7 μW/cm^2 was slightly lower, which was found to be negatively affected by the ascorbate in tear. Instead of using Au electrode, Reid et al. [121] employed a carbon paste containing graphite and CNT as bioelectrode. They also chose lactate in tear as fuel by modifying the anode with lactate oxidase, and the power density of 2.4 μW/cm^2 was slightly improved. To figure out the reason behind cathode performance limitation, a computational model was built in their work, which discovered that large portion of the CNT surface was not effectively connected to the enzyme. They also tried the bucky paper as electrode to support the lactate dehydrogenase for anode and bilirubin oxidase for cathode [122]. This time, a much-improved power density of 8 μW/cm^2 was demonstrated, but the discharge stability was not satisfactory, which decreased rapidly in the first 4 h. Also, the similar characteristic of CNT with asbestos may also cause safety concerns. In summary, the contact lenses-based fuel cell technology is still hindered by its limited power output as well as operation lifetime. The safety issue is another great concern considering its intimate contact with the eyeball.

4.1.2. Tattoo-based cells

Tattoo-based cell is another trend in the early development of wearable enzymatic fuel cells, which has an intimate contact with skin to receive fuel from sweat efficiently. Jia et al. [123] first proposed this type

Table-5
Summary of flexible enzymatic fuel cells reported in literature.

Reference	Anode	Fuel	Electrolyte	Oxidant	Cathode	OCV	Power density	Durability	Flexibility
Contact lenses-based									
Falk et al. [118]	CDH || Au	Glucose	Tear	Dissolved O_2	BOx || Au	0.57 V	1 μW/cm^2	20 h (0.51 V)	
Falk et al. [119]	TTF-TCNQ || Au	Ascorbate	Tear	Dissolved O_2	BOx || Au	0.54 V	3.1 μW/cm^2	6 h (0.4 V)	
Xiao et al. [120]	LOx || Au	Lactate	Synthetic tear	Dissolved O_2	BOx || Au	0.38 V	1.7 μW/cm^2	5.5 h (0.15 V)	
Reid et al. [121]	LOx ||C paste	Lactate	Synthetic tear	Dissolved O_2	BOx ||C paste	0.44 V	2.4 μW/cm^2		
Reid et al. [122]	LDH || buckypaper	Lactate	Synthetic tear	Dissolved O_2	BOx || buckypaper	0.41 V	8 μW/cm^2	17 h (0.2 V)	
Tattoo-based									
Jia et al. [123]	LOx	Lactate	Sweat	Air	Pt ||C	0.5 V[a]	44 μW/cm^2	4 weeks	Bending; Stretching; twisting
Bandodkar et al. [124]	LOx || CNT-NQ || Au	Lactate	Buffer solution	Ag_2O	Ag_2O/CNT || Au	0.5 V	1.2 mW/cm^2	2 days	Stretching
Chen et al. [125]	LOx || buckypaper	Lactate	Phosphate buffer	O_2	BOx || buckypaper	0.74 V	520 μW/cm^2	48 h (0.55V)	Stretching (100 times)
Sun et al. [126]	AOx || N-doped C aerogel	Ethanol	Sweat	Dissolved O_2	BOx || N-doped C aerogel		1 μW/cm^2	70 min	wearable
Textile-based									
Kwon et al. [127]	GOx || MWCNT yarn	Glucose	Buffer solution	Dissolved O_2	BOx || MWCNT yarn	0.7 V	2.18 mW/cm^2	48 h (0.4V)	Woven into textile
Jia et al. [128]	LOx	Lactate	Buffer solution	Air	Pt	0.67 V	100 μW/cm^2	6 h	Stretching; Bending (100 times)
Jeerapan et al. [129]	GOx	Glucose	Phosphate buffer	Ag_2O	Ag_2O/Ag	0.44 V	160 μW/cm^2		Stretching; Indentation; Twisting (100 times)
	LOx	Lactate				0.46 V	250 μW/cm^2		
Wang et al. [130]	GOx	Glucose	Phosphate buffer	Air	Prussian blue	0.3 V	16.7 μW/cm^2	240 min	wearable
Paper-based									
Shitanda et al. [131]	LOx ||C paste	Lactate	Phosphate buffer	Air	BOx ||C paste	0.6 V	113 μW/cm^2	1.5 h	On arm
Shitanda et al. [132]	GDH ||C paste	Glucose	Phosphate buffer	Air	BOx ||C paste	0.76 V	170 μW/cm^2		On diaper
Gel electrolyte									
Ogawa et al. [133]	FDH || CNT-coated textile	Fructose	McIlvaine buffer solution	Air	BOx || CNT-coated textile	0.74 V[a]	200 μW/cm^2		Stretching; Twisting; Wrapping
Hui et al. [134]	GOx || Au-coated Ni foam	Glucose	Agarose gel	Air	Laccase || Au-coated Ni foam	0.58 V	2.3 mW/cm^2	60 days	Bending (1000 times)
Yin et al. [135]	GDH ||C fiber	Glucose	Hydrogel	Air	BOx ||C fiber	0.51 V	216 μW/cm^2	72 h	Sewed into cloth
Kong et al. [136]	GDH || N-doped graphene	Glucose	PVA gel	Air	BOx || N-doped graphene	0.45 V	27 μW/cm^2	20 days (OCV)	Bending (100 times)
Suzuki et al. [137]	GDH || GMgOC-C cloth	Glucose	Hydrogel	Air	BOx || MgOC–C cloth	0.82 V	420 μW/cm^2	2.5 h (0.4V)	
Chen et al. [138]	GOx || G-CNT	Glucose	Hydrogel	Air	BOx || G-CNT	0.65 V	64.2 μW/cm^2		Bending (400 times); Stretching
Yang et al. [139]	LOx – MWCNT/NQ ||C cloth	Lactate	PVA gel	Air	Pt/C ||C cloth	0.5 V[a]	62.2 μW/cm^2	12 h	Bending; Twisting

AOx: alcohol oxidase; BOx: bilirubin oxidase; CDH: cellobiose dehydrogenase; FDH: fructose dehydrogenase; GDH: glucose dehydrogenase; GOx: glucose oxidase; LOx: lactate oxidase; LDH: Lactate dehydrogenase; NQ: naphthoquinone.
[a] Estimated from the figure of corresponding reference.

of fuel cell, which could be attached conformally on skin and consumed lactate from sweat via its lactate oxidase-based anode. As for the cathode, an inorganic catalyst of Pt was still adopted for the reduction of oxygen from ambient air. This epidermal fuel cell output a peak power density of 44 μW/cm^2, which could be operated for 4 weeks before degradation. Bandodkar et al. [124] further improved the power density of tattoo-based enzymatic fuel cell by developing an innovative "island--bridge" cell configuration. As shown in Fig. 11b, the cell electrodes were deposited on circular islands which were tightly bonded to the stretchable substrate beneath them, while the connection of them was realized by serpentine bridges which were free to deform when encountering external stress. With lactate oxidase in anode and Ag_2O in cathode, their cell output a peak power density as high as 1.2 mW/cm^2, which could be used for powering a Bluetooth low-energy radio. Chen et al. [125] also adopted the "island-bridge" configuration and used bucky paper as electrode to support the lactate oxidase at the anode and bilirubin oxidase at the cathode. The power density of 520 μW/cm^2 was as not as high as the previous work, which was mainly due to the weaker activity of the lactate oxidase cathode than Ag_2O. However, since ambient air was used as oxidant rather than the stored Ag_2O, this cell has a better potential for long-term operation. In addition to lactate and glucose, the human sweat may also contain ethanol if the individual drinks alcohol, which can be utilized by the enzymatic fuel cell for either alcohol detection or electricity generation. Sun et al. [126] used alcohol oxidase as anode catalyst and bilirubin oxidase as cathode catalyst, both of which were supported on the nitrogen-doped carbon aerogel. Performance of the cell on human skin under different alcohol ingestion scenarios were studied, but the peak power density only reached 1 μW/cm^2. This lower performance

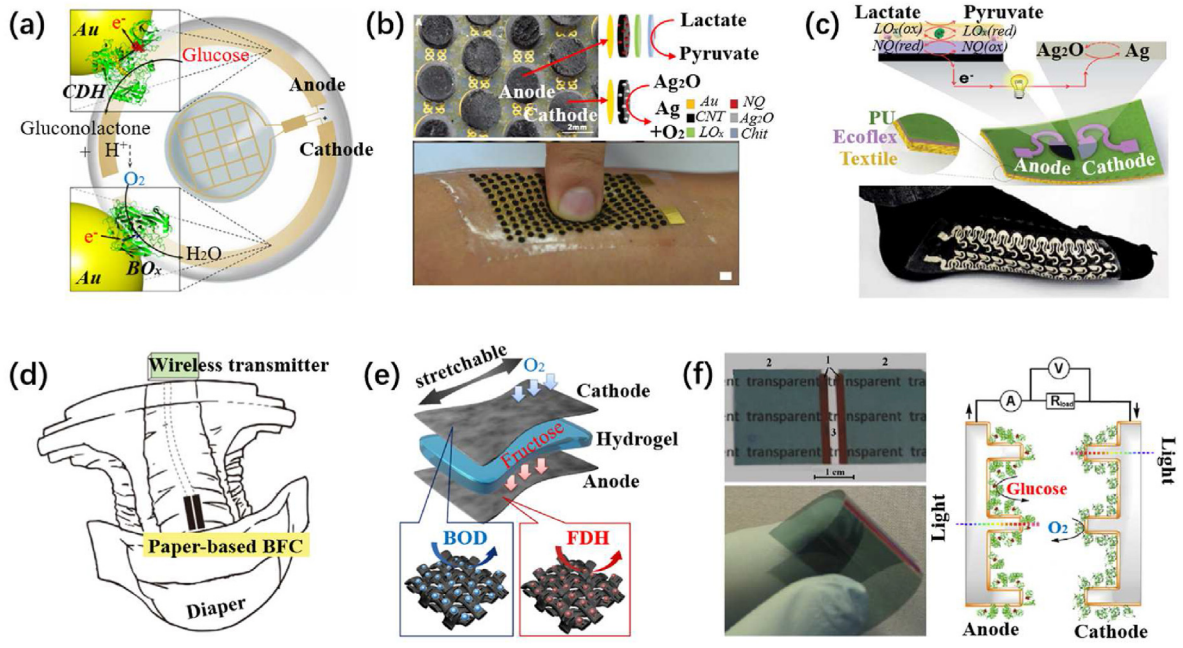

Fig. 11. Flexible enzymatic fuel cells based on different substrates: (a) Contact lenses-based cell (Reproduced with permission from Elsevier [118]); (b) Tattoo-based cell (Reproduced with permission from RSC [124]); (c) Textile-based cell (Reproduced with permission from RSC [129]); (d) Paper-based cell (Reproduced with permission from ACS [132]); (e) Gel electrolyte-based cell (Reproduced with permission from Elsevier [133]); (f) Plastic film-based cell (Reproduced with permission from Elsevier [117]).

compared with lactate and glucose is probably due to the lower concentration of ethanol in sweat.

4.1.3. Textile-based cells

Despite their convenience, the contact lenses-based and tattoo-based enzymatic fuel cells may cause eye or skin irritation in long-term operation, whose electrode area is also strongly restricted. On the other hand, the enzymatic fuel cell can be fabricated in large-area textiles by adopting either planar-shape or fiber-shape electrodes. Kwon et al. [127] used the biscrolled CNT yarn as enzyme supporter and weaved them into a textile. Glucose oxidase was used to extract energy from human serum while bilirubin oxidase was used to reduce oxygen, and a peak power density as high as 2.18 mW/cm^2 was achieved. Jia et al. [128] built their enzymatic fuel cell on a wearable textile such as a headband or a wristband, which was successfully demonstrated for powering a LED or a digital watch using sweat lactate. A moderate power density of 100 μW/cm^2 was achieved, and the cell could be stretched and bended for 100 times. Jeerapan et al. [129] fabricated textile-based enzymatic fuel cell on socks with high stretchability by using the screen-printing technique (Fig. 11c). For the anode side, either lactate oxidase or glucose oxidase was used as bio-catalyst, while Ag_2O was used as the oxidant which can be reduced to Ag during discharge. Benefited from the conductive inks as well as the serpentine cell design, their cell could tolerate various deformations including stretching, twisting and indentation. The power output reached 160 and 250 μW/cm^2 for the glucose and lactate fuel, respectively. Furthermore, Wang et al. [130] employed a moisture management fabric for the flexible enzymatic fuel cell, which could promote the flow speed of reactants inside and the associated molecular transport. Compared with filter paper or cotton substrate, this cell achieved a better power output of 16.7 μW/cm^2, but the OCV of 0.3 V was relatively limited.

4.1.4. Paper-based cells

In addition to textile, cellulose paper has also been used as substrate for flexible enzymatic fuel cells, which can be either attached directly on skin or integrated into other wearable stuff. Recently, Shitanda et al. [131] developed a paper-based lactate fuel cell stack with high absolute power output. To ensure a clear oxygen diffusion path through the paper, water repellent coating was conducted to the paper substrate, while an extra fuel supply paper was covered on the printed electrodes. When attached to the arm, such a 6 x 6 stack (6 cells in series and 6 cells in parallel) could provide an OCV of 3.55 V and a power output of 4.3 mW by using human sweat, which were sufficient to power a wireless transmission device. They also developed a paper-based glucose fuel cell and integrated into a diaper (Fig. 11d) [132]. By using glucose dehydrogenase as anode catalyst, this wearable fuel cell could sense the concentration of urine sugar in the range of 0–10 mM, and transmit the result wirelessly to a cellphone without external power input.

4.1.5. Gel-electrolyte cells

Despite their inability of uninterrupted operation, the utilization of gel electrolyte can store a higher concentration of fuel than that in natural tear or sweat, so that an improved cell performance is guaranteed. Moreover, it can still function normally when no fuel is available from the body. Ogawa et al. [133] employed a fructose-containing hydrogel film as electrolyte, which was sandwiched between two layers of CNT-deposited textile electrodes (Fig. 11e). Fructose dehydrogenase was used as bioanode catalyst, and the power density of 200 μW/cm^2 was not as high as previous cells, which could be related to the sluggish fructose oxidation reaction. Hui et al. [134] used agarose to gel the glucose fuel, which was next coated into a cellulose acetate membrane to serve as electrolyte. As for electrodes, Au-coated Ni foam was used as catalyst supporter, which were dip-coated in glucose oxidase solution and laccase solution to form the anode and cathode, respectively. Benefited from the sufficient assembling pressure, a superior power density of 2.32 mW/cm^2 was obtained, which could be maintained for 60 days with only 15.4 % loss. Yin et al. [135] used CNT-coated carbon fiber to support the glucose dehydrogenase and bilirubin oxidase, respectively, which could be woven into textile and produce electricity when contacting sweat. Nevertheless, the cell performance was tested by simply putting the fiber electrodes on a gel electrolyte without effective packaging, which achieved a power density of 216 μW/cm^2. Kong et al. [136] employed the direct laser writing technique to prepare N-doped graphene electrode on a polyimide film precursor, which was next incubated with the corresponding enzyme. A PVA-based gel electrolyte was then covered onto the

electrodes. However, the power output of 27 μW/cm^2 was relatively low, which could be due to the elongated ionic path as well as the lower glucose concentration. Suzuki et al. [137] used dopamine methacrylamide-based hydrogel to store the glucose fuel, which was attached to bioelectrodes to form the fuel cell. A high power density of 420 μW/cm^2 was obtained, which dropped to 330 μW/cm^2 after 2.5 h' discharge at 0.4V. Chen et al. [138] developed a stretchable enzymatic fuel cell based on textile electrodes and a polyacrylamide-based hydrogel electrolyte. An optimized power density of 64.2 μW/cm^2 was obtained, and the cell refueling was also demonstrated successfully for four times, proving that gel-electrolyte cells can also work continuously upon in-time refueling. Furthermore, the cell can retain most of its performance even after 400 times' bending or 60 % stretching. Yang et al. [139] modified the lactate bioanode with multi-walled CNT and naphthoquinone, which could promote the electron transfer rate between the catalytic site and the current collector. The cell also employed the sandwich structure with a PVA-based gel electrolyte in between, which could function in both external lactate supply mode and pre-stored lactate mode. The power density was 62.9 and 49.3 μW/cm^2, respectively, which could withstand bending and torsion deformations.

4.2. Microbial fuel cells

Instead of using enzyme catalysts, microbial fuel cell generally employs bacterial in the anode to oxidize organic fuels, and inorganic catalyst in the cathode to reduce the ambient air, while a nutrient solution is adopted as both fuel and electrolyte. Table-6 summarizes recent research works on flexible microbial fuel cells. Due to the sluggish and complex reactions inside the bacterial cell, the power density is much lower than enzymatic fuel cells, which is generally around several μW cm^{-2}. Nevertheless, this low-cost fuel cell technology can still provide sufficient power for some microwatt applications, such as wearable sensors. To date, different substrate materials have been adopted for developing flexible microbial fuel cells as shown in Fig. 12. Early studies employed PDMS [140] or rubber [141] material to serve as the channel (Fig. 12a), which achieved quite limited power density less than 1 μW/cm^2. Later on, porous and hydrophilic substrates such as paper and textile were more frequently adopted. Moreover, tubular microbial fuel cells were also reported.

4.2.1. Paper-based cells

Paper can serve as the electrolyte container for flexible microbial fuel cells, absorbing either a polymer electrolyte or a culture medium for ionic connection purpose. On its two side, carbon-based electrodes are generally used for bacterial supporting, such as carbon cloth. Fraiwan et al. [142] infiltrated the paper substrate with sodium polystyrene sulfonate to fabricate a paper-based PEM, which was sandwiched by carbon cloth electrodes (Fig. 12b). Shewanella oneidensis was used for anode to consume the nutrition in the L-broth, while ferricyanide was directly used as oxidant for the cathode. The obtained power density of 5.5 μW/cm^2 was quite high in the beginning, which however dropped significantly within 15 min. By adopting multiple anodes stacked one by one and a Nafion membrane electrolyte, they further improved the power density to 28.4 μW/cm^2, which was mainly attributed to the increased area for bacterial inoculation [143]. The operation lifetime was also elongated to 200 min.

With an extra layer of carbon ink deposition, the paper substrate could also serve as electrodes without the need for carbon cloth, leading to a monolithic cell structure. Veerubhotla et al. [144] used pencil-stroked graphite on paper as bio-electrodes and blank paper as the electrode separator. Shewanella putrefaciens was deposited onto the graphite anode together with lactate fuel, and the cell was activated

Table-6
Summary of flexible microbial fuel cells reported in literature.

Reference	Anode	Fuel	Electrolyte	Oxidant	Cathode	OCV	Power density	Durability	Flexibility
Paper-based cells									
Fraiwan et al. [142]	MR-1 ||C cloth	L-broth	Paper-based PEM	Ferricyanide	C cloth	0.32 V	5.5 μW/cm^2	15 min	
Fraiwan et al. [143]	MR-1 ||C cloth	L-broth	Nafion 117	Ferricyanide	C cloth	0.37 V	28.4 μW/cm^2	200 min	
Veerubhotla et al. [144]	S. putrefaciens || Graphite	Lactate media		Air	Graphite	0.4 V	0.88 μW/cm^2	500 min	
Fraiwan et al. [145]	MR-1 ||C	L-broth	Paper-based PEM	Ferricyanide	C	0.4 V[a]	1.27 μW/cm^2	20 min	
Veerubhotla et al. [146]	S. putrefaciens || eyeliner ink	L-broth		Air	Eyeliner ink	0.4–0.5 V[a]	1.25 μW/cm^2[a]	50 min	
Mohammadifar et al. [147]	MR-1 || activated C & graphite	L-broth	Wax-based CEM	Air	activated C	0.5 V[a]	0.46 μW/cm^2		
Jayapiriya et al. [148]	*E. coli* || Ag ink	L-broth		Air	MnO_2 ||C ink	0.48 V	11.8 μW/cm^2	70 min	
Textile-based cells									
Pang et al. [149]	PAO1 || PEDOT:PSS	L-broth		Ag_2O	Ag_2O || PEDOT:PSS	0.3 V[a]	1.0 μW/cm^2		Stretching (70cycles); Twisting
Pang et al. [150]	PAO1 || PEDOT:PSS	L-broth		Ag_2O	Ag_2O || PEDOT:PSS	0.4 V[a]	6.4 μW/cm^2		Stretching; Twisting
Ryu et al. [151]	MR-1 || PEDOT:PSS, DMSO, PEI	L-broth		Ag_2O	Ag_2O || PEDOT:PSS	0.37 V	47.2 μW/cm^3		Bending; knotting; looping; winding
Pu et al. [152]	Bacterium || C–Ti foil	Wastewater		Air	Pt/C ||C cloth	0.6 V[a]	25 μW/cm^2		
Tubular cells									
Taghavi et al. [153]	Microbial ||C sleeve	Urine	Nafion	Air	Microbial ||C sleeve		4 μW/cm^2[a]	70 days	Bending
Yu et al. [154]	*Escherichia coli* || N–MoO_{3-x}-coated C fiber	Nutrients	CEM	Air	Pt/C	0.3 V[a]	0.61 mW/cm^3	100 h	Bending

AOx: alcohol oxidase; BOx: bilirubin oxidase; CDH: cellobiose dehydrogenase; GDH: glucose dehydrogenase; GOx: glucose oxidase; LOx: lactate oxidase; NQ: naphthoquinone; PAO1: pseudomonas aeruginosa; PB: prussian blue; MR-1: shewanella oneidensis.

[a] Estimated from the figure of corresponding reference.

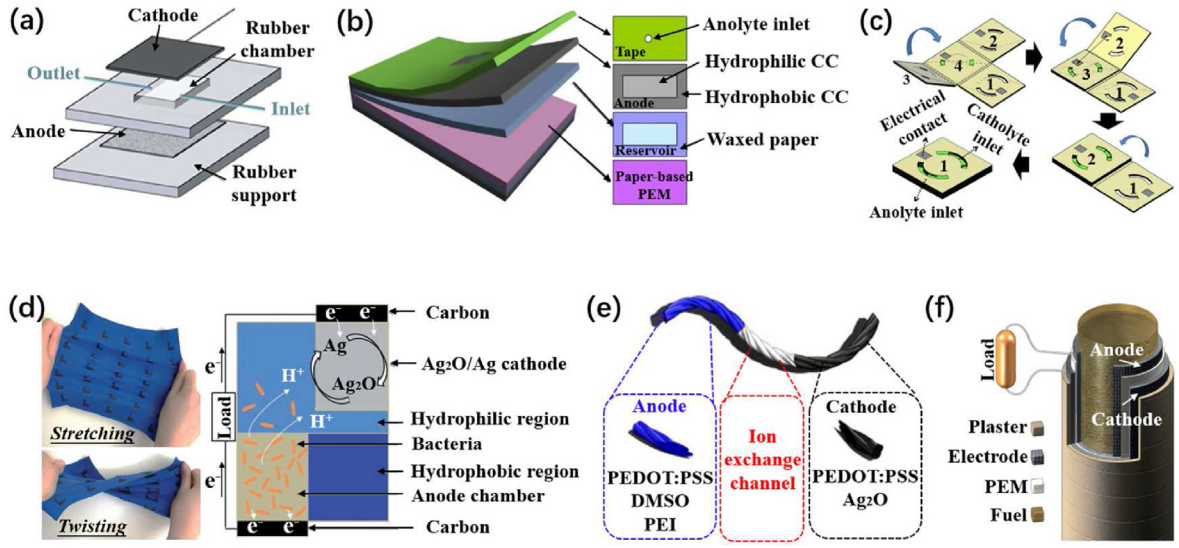

Fig. 12. Flexible microbial fuel cells based on different substrates: (a) Plastic-based cell (Reproduced with permission from Wiley [141]); (b) Paper-based cell (Reproduced with permission from Elsevier [142]); (c) Paper-based stack with an origami design (Reproduced with permission from Elsevier [145]); (d) Textile-based cell with printed planar electrodes (Reproduced with permission from Wiley [150]); (e) Textile-based cell with fiber-shape electrodes (Reproduced with permission from Elsevier [151]); (f) Tubular cell (Reproduced with permission from Wiley [153]).

quickly within 10 s. A peak power density of 0.88 μW/cm^2 was calculated based on the anode area, and the cell could be discharged stably for 500 min with continuous capillary fuel supply. They also employed eyeliner ink to paint the carbon electrodes on paper, which was next inoculated with Shewanella putrefaciens as the bioanode [146]. The generated power density was about 1.25 μW/cm^2 based on the anode area, and a discharge lifetime of 50 min was achieved at 3.8 μA cm^{-2}. To sum up, the deposited carbon electrode is still inferior to the independent carbon cloth, which is mainly due to its lower electric conductivity.

The foldability of paper also enables convenient microbial fuel cell stacking through the art of origami. Fraiwan and Choi [145] developed a 4-cell paper-based microbial fuel cell stack by a simple folding process. As shown in Fig. 12c, the carbon electrodes and PEM were deposited into the paper substrate first, and the single cells were automatically connected in series during folding. With Shewanella oneidensis for anode and ferricyanide for cathode, their stack delivered a high OCV of 1.6 V, and the power density was 1.27 μW/cm^2. However, two clips were still needed for tight assembling, which was an obstacle to the device flexibility. Mohammadifar et al. [147] also used the origami technique to develop paper-based microbial fuel cell. Five different anode materials were compared in terms of OCV and power generation, and the graphite ink with activated carbon was proved to be the best. Jayapiriya and Goel [148] developed an origami-based microbial fuel cell as well. The hydrophobic barriers were deposited on paper first by 3D printing, followed by the drop-casting of anode and cathode inks. With E. Coli as the anode bacterial and MnO_2 as the cathode catalyst, a high power density of 11.8 μW/cm^2 was demonstrated, and the paper substrate with small pore size and nominal thickness was found to be beneficial to the mass transport.

4.2.2. Textile-based cells

The textile substrate generally has a better flexibility than paper especially in terms of stretchability. Using textile as substrate, Pang et al. [150] screen printed 35 microbial fuel cells on a 19 cm × 19 cm area at one time, proving that microbial fuel cells could be mass produced with low cost (Fig. 12d). PEDOT:PSS and carbon inks were used for current collection, while pseudomonas aeruginosa and Ag_2O was used for the anode and cathode reactions, respectively. Their textile-based cell could be stretched and twisted, generating a power density of 6.4 μW/cm^2. In another work, they used separate textile substrates for the anode and cathode deposition, and combined them together by applying adhesive to the electrode periphery [149]. A conductive thread was also sewed into the anode for current collection purpose. However, the power density of 1 μW/cm^2 was lower, which could be due to the insufficient contact between anode and cathode where adhesive was not applied. Unlike the direct electrode printing on textile, Ryu et al. [151] developed a fiber-shape microbial single cell first by depositing Shewanella oneidensis on one end of a yarn and Ag_2O on the other end (Fig. 12e). In the middle, a blank section was remained to separate the electrodes. Afterwards, the 1D fiber cell could be further woven into 2D and 3D textiles, generating much higher voltage and power output. The textile-based flexible microbial fuel cell has also been applied for municipal wastewater treatment [152].

4.2.3. Tubular cells

Tubular microbial fuel cell studies were quite scarce at the moment. Taghavi et al. [153] developed a concentric tubular cell by using a Nafion membrane tube as electrolyte and two carbon fiber sleeves as electrodes (Fig. 12f). The microbes were inoculated into the electrodes by using activated anaerobic sludge, and human urine was flowed into the tube to provide urea fuel to the anode side. The power density was about 4 μW/cm^2, and the cell could be operated continuously for 70 days with the help of a waterproof plaster package. Yu et al. [154] also developed a tubular microbial fuel cell using a N and low-valence-state Mo dual-doped MoO_3 nanowire as fiber anode. A cation exchange membrane was used to separate the anode and the Pt/C cathode, which were all sealed in a heat-shrinkable tube. When *Escherichia coli* and air were provided into the tube separately, the bendable cell could deliver a power density of 0.61 mW/cm^3.

5. Other flexible fuel cells

In addition to flexible PEMFCs, MFCs and BFCs, other types of FFCs have also been proposed recently, such as the solid oxide fuel cell, photocatalytic fuel cell and liquid metal fuel cell. However, the relevant reports are quite scarce at the moment, which are still in early R&D stage.

5.1. Flexible solid oxide fuel cell

As a high-temperature fuel cell technology working at 600–1000 °C, solid oxide fuel cell (SOFC) made of ceramic materials is more

appropriate for stationary applications rather than portable devices, not to mention wearable electronics. Nevertheless, the idea of flexible SOFC still interests some researchers, which has great advantage in mechanical strength during both stack assembling and thermal cycling. Due to the brittle nature of ceramic materials, SOFC single cells tend to crack during stacking, which is especially the case for large electrode areas. On the other hand, the repetitive heating and cooling during operation will induce thermomechanical shock to the cells. Regarding this, a thin-film SOFC with certain degree of flexibility will benefit the mechanical strength of the whole system. Cho and Choi [155] fabricated a 0.2 mm-thick SOFC supported on a porous Ni film, which was prepared by the mold casting of Ni powders. Classic yttria stabilized zirconia (YSZ) electrolyte and Ni-YSZ anode were next coated on the Ni support, followed by the screen printing of lanthanum strontium cobalt iron oxide (LSCF) cathode. Benefited from the high temperature operation, a peak power density of 470 mW/cm^2 was reported, but the cell flexibility was not demonstrated. Later on, they further proposed a NiFe-supported thin-film SOFC, and compared its flexibility with the conventional anode- or electrolyte-supported cell [156]. Through a 3-point bending test, it was found that the cell with NiFe metal support reduced at 1000 °C achieved the highest flexibility, which could be bent continuously without any serious destruction. On the contrary, the anode- and electrolyte-supported cells both cracked after only a small deformation. Instead of metal foil support, Jeon et al. [157] recently developed a bendable YSZ electrolyte film via the tape-casting process. The anode and cathode pastes were next screen-printed onto the opposite sides of it, followed by a cofiring process. When facing thermal shocks during on-off cycle test, their cell exhibited a stable output for 500 h with only 4.3 % degradation. Won et al. [158] reported a phase-controlled 3YSZ electrolyte which sacrificed the ionic conductivity for higher mechanical strength. The ultrathin 3YSZ electrolyte with a thickness of 22 μm is highly bendable, leading to a 60 μm thick flexible SOFC with a peak power density as high as 860 mW/cm^2 at 900 °C. To sum up, the study on flexible SOFCs at the moment is mainly targeted for improving mechanical strength rather than applying them in a deformative environment.

5.2. Flexible photocatalytic fuel cell

Instead of metal catalyst or biocatalyst for the anode side, photocatalyst such as the classic TiO_2 has also been employed for fuel oxidation, leading to a photocatalytic fuel cell which can work under light irradiation. As for wearable applications, a few researchers tried to develop flexible photocatalytic fuel cells which can either fueled by the body fluid or the external environment. Lui et al. [159] developed a planar cell based on a TiO_2 anode and a Pt/C cathode, while a cellulose paper was used as electrolyte container. When using different types of organic fuels such as lactic acid, ethanol, methanol, glycerol, urea and glucose, it was found that the lactic acid fuel achieved the highest power output of 18.4 mW cm^{-2} g^{-1}, and the cell performance was only marginally decreased in the bending situation. Furthermore, this photocatalytic fuel cell was successfully integrated into a sweatband. To utilize mine gas, Yang et al. [160] developed a tubular cell which had a graphene fiber inside as air cathode, a TiO_2-deposited graphene spring outside as photoanode, and a PVA gel electrolyte in between. Under the simulated sunlight irradiation, 2.0 vol% methane in the mine gas could be effectively oxidized at the photoanode, generating a power density of 40 mW/cm^2. Furthermore, the current output barely changed when it was bent from 0 to 180°. Despite their potentially higher energy efficiency, the operation stability of flexible photocatalytic fuel cells could be a problem due to its strong correlation with the light intensity.

5.3. Flexible liquid metal fuel cell

When solid metal is used as fuel in a “fuel cell”, it lacks the key ability of uninterrupted operation due to the inability of continuous metal supply, which is more commonly referred as “metal-air battery”. However, some metal alloys are in liquid status even at room temperature, which can be flowed in and out continuously, leading to a liquid metal fuel cell. Till now, the study on its flexible version is very limited. Xiong et al. [161] employed the eutectic gallium-indium alloy as both fuel and anode, which had a melting point of ~15.3 °C. With a polyacrylic acid and KOH based gel electrolyte, such a special fuel cell could provide a power density of 72.8 mW/cm^2, and the high flexibility was guaranteed by its rubber container. Nevertheless, the employment of liquid metal fuel will inevitably increase the system weight compared with either hydrogen or hydrocarbon fuel, which is less competent for wearable applications.

6. Conclusion & future perspectives

From the above discussion, it can be concluded that FFC is still in its infancy stage, which is advantageous for its uninterrupted operation ability. In literature, three major types of FFC technology have been developed, including the flexible PEMFC, MFC and BFC. Their research highlights and major gaps are summarized in below, respectively, together with a comparative analysis of their suitability for different application scenarios.

- For the flexible PEMFC, a planar cell structure originated from its rigid counterpart is still the mainstream, and the key to high flexibility lies in the material of BPP, GDL and other auxiliary components. Metal-coated polymers such as Au-PDMS and Ag-PDMS are popular for developing flexible BPPs, while carbon fiber-based GDLs such as carbon cloth and CNT membrane generally have a satisfactory performance against bending deformation. Specifically, the thin-film PEMFC can better accommodate on-body missions due to its improved conformality, but the assembling pressure is inevitably sacrificed. As from the fuel point of view, most existing studies prefer hydrogen so that a high power density of ~100 mW/cm^2 can be delivered. However, flexibility of the gas supply subsystem is rarely studied, which will be the main obstacle to its on-body application. Alternatively, hydrocarbon fuel such as ethanol may be a better choice, which is much safer to wear and can be supplied passively by capillary action or vapor feeding. To overcome its sluggish oxidation, an alkaline polymer electrolyte is preferred, but the carbonation issue would be another problem for its long-term stability. Also, oxidation intermediates such as CO may further poison the catalysts. In addition to the mainstream planar cell, tubular cell has also been investigated for flexible PEMFC, which generally adopts a concentric MEA with anode inside and cathode outside. Since fuel is provided inside the tube, no BPP is needed any more, while the concentric structure can provide sufficient stress for cell assembling. However, tubular cells are more difficult to fabricate and are less stable than planar cells with BPP, which may be choked when facing external deformations.
- For the flexible MFC, a micro channel is utilized for liquid electrolyte delivery instead of a PEM, which can be either engraved in a plastic chip or formed by multiple fibers/threads. The former case is by nature a thin version of conventional rigid MFCs, which generally requires an active pump to control the electrolyte flow rate accurately. By adopting capillary action instead of pumping, paper-based fuel cells can have a greatly simplified system, whose cell components are all integrated in a single piece of paper. Their fabrication can also be accomplished by low-cost and efficient printing techniques. However, cellulose paper is vulnerable to repetitive deformation especially in wet condition, which calls for substitutive paper-like materials such as cotton and sponge. A delicate control of the capillary flow should also be accomplished in order to achieve high energy efficiency and long discharge lifetime, which calls for in-depth study of the relationship between mass transport rate and paper micropore structure. Furthermore, most paper-based MFC studies in literature still employ plastic supports and pay little attention to the system flexibility,

which worth further investigation in the future. In addition to the above two planar cell designs, thread-based tubular MFCs are also attractive, which can be further sewed into clothes. Unlike the concentric structure in tubular PEMFCs, a parallel configuration with one thread for anode, another thread for cathode and a third one for separation is generally adopted, which are all encapsulated in a tube shell. Similarly, the fabrication difficulty and choking issue impede its practical application.

- For the flexible BFC, since the fuel and electrolyte can be provided by human body, the cell structure can be simplified to two bioelectrodes only. Typical examples include the contact lenses-based cell mounted on eyeball and the tattoo-based cell attached on skin, which can utilize lactate or glucose directly from the tear and sweat, respectively. Alternatively, a textile or paper substrate can be used to support bioelectrodes and store biofluids, ensuring a better operation stability as well as breathability to the skin. According to the nature of biocatalyst, flexible BFCs can be divided into enzymatic fuel cell and microbial fuel cell, of which the former can achieve several hundred $\mu W\ cm^{-2}$ while the latter only delivers several $\mu W\ cm^{-2}$. On the other hand, the microbial fuel cell can achieve a better long-term durability than the enzymatic fuel cell, which also has a much lower fabrication cost. Consequently, the technology should be selected according to the detailed application in terms of rated power and device lifetime. When facing practical applications, the durability of enzyme/microbe needs to be significantly improved before they can compete with abiotic fuel cells. In addition, the safety concern on biocatalysts may be another obstacle especially for the microbial fuel cell. Furthermore, similar to all energy harvesting technologies, the power output stability of BFC is not as good as PEMFC and MFC with constant fuel supply due to the variation of human body physiological status, so that an energy storage component such as battery or supercapacitor may be required, which will complicate the whole energy system.
- From the above summary, it is recommended that flexible PEMFCs are more suitable for high-power wearable equipment, such as smart watches, glasses, backpacks and shoes. These smart devices are currently powered by Li-ion batteries, while the flexible PEMFC can provide them a much longer operation time especially in outdoor missions. Flexible MFCs, especially paper-based and thread-based ones, are more appropriate for medium-power applications such as various wearable body sensors. These healthcare devices call for lightweight yet durable power sources, while the flexible MFC fabricated on paper or cloth well meets this requirement, which can also be instantly refueled without blackout. As for flexible BFCs, they may be suitable for low-power sensing devices such as electronic skins and contact lens. These devices are in direct contact with the human body, so that the fuel can be smoothly provided from sweats or tears.

Despite 20 years' research efforts, in order to compete in the future market of flexible power sources, several key technical and economic targets need to be achieved for the FFC technology, including the discharge performance, energy density, device lifetime and capital cost. For the first indicator, since the power requirement from wearable electronics is generally limited, ranging from several $\mu W\ cm^{-2}$ to $mW\ cm^{-2}$, current FFCs can already achieve this goal. The key issue lies in the limited voltage of fuel cell (generally less than 1 V), which should be stacked to provide a more practical voltage. For the energy density, the FFC holds a great advantage against other technologies, which can reach beyond 1000 $Wh\ kg^{-1}$. Nevertheless, this is based on the premise of continuous fuel supply. In real applications, when a limited fuel cartridge is used and coupled with the fuel cell main body, the system energy density will be discounted due to the significant weight ratio of the latter. In general, a twice value of current Li ion batteries should be accomplished in order to sustain certain competitiveness (i.e. 500 $Wh\ kg^{-1}$). For the device lifetime, state-of-the-art stationary fuel cells can reach 40000 h. However, this value will be shortened for FFCs due to frequent cell deformation, which will undermine both the catalyst attachment and the channel structure gradually. In general, a moderate lifetime comparable with current Li ion batteries should be achieved at least, such as 20000 h of continuous operation. As for its capital cost, the FFC is potentially cheaper than conventional fuel cells due to the elimination of metal-based BPPs and the potential utilization of non-noble catalysts. Therefore, its market price target should also be set at the same level with other flexible power sources.

To achieve the above targets, future FFCs should be further optimized in aspects of material, structure as well as manufacture method. To improve the voltage output, FFC stacking is worth investigating, of which the effect of stack deformation on cell connection and species distribution is especially important. Moreover, novel stack structures should be invented to avoid sacrificing its flexibility. To improve the energy density, more lightweight materials for structural support (e.g. BPP, channel wall and cell package) should be discovered, and the thickness needs to be reduced as much as possible without breaking the assembling pressure threshold. In addition, passive mass transport via integrated capillary structure is a promising direction to replace active pumps inside the system. To improve the device lifetime, more robust ionic binders should be utilized to better fix the catalyst particles on current collector, while surface treatment to the current collector can also be applied before catalyst deposition. Moreover, mechanical strengthening of the local structure can be applied to cell parts with heavy deformation burden. Finally, to control the capital cost, non-noble metal catalyst is the most important direction considering the fact that wearable electronics generally have moderate requirement of power density. On the other hand, developing a low-cost yet efficient fabrication method for FFC large-scale manufacture is also meaningful. For instance, the ink printing method (roll-to-roll, screen or inkjet printing based on the production scale) is especially advantageous for the deposition of electrodes and current collectors.

Declaration of competing interest

The authors declare that they have no known competing financial interests or personal relationships that could have appeared to influence the work reported in this paper.

Acknowledgement

The authors would like to acknowledge support from National Natural Science Foundation of China (52206240), Natural Science Foundation of Guangdong Province (2023A1515012947), and Shenzhen Science and Technology Innovation Commission (GXWD20220811163936002, SGDX20210823103537038).

References

[1] R. O'hayre, S.-W. Cha, W. Colella, F.B. Prinz, Fuel cell fundamentals, John Wiley & Sons (2016).
[2] T. Wilberforce, A. Alaswad, A. Palumbo, M. Dassisti, A.-G. Olabi, Advances in stationary and portable fuel cell applications, Int. J. Hydrogen Energy 41 (2016) 16509–16522.
[3] W.S. Wong, A. Salleo, Flexible electronics: materials and applications, Springer Sci. Bus. Media (2009).
[4] X. Fan, B. Liu, J. Ding, Y. Deng, X. Han, W. Hu, et al., Flexible and wearable power sources for next-generation wearable electronics, Batter. Supercaps 3 (2020) 1262–1274.
[5] S. Mukherjee, A. Albertengo, T. Djenizian, Beyond flexible-Li-ion battery systems for soft electronics, Energy Storage Mater. 42 (2021) 773–785.
[6] Q. Liu, Z. Chang, Z. Li, X. Zhang, Flexible metal–air batteries: progress, challenges, and perspectives, Small Methods 2 (2018) 1700231.
[7] S. Palchoudhury, K. Ramasamy, R.K. Gupta, A. Gupta, Flexible supercapacitors: a materials perspective, Front. Mater. 5 (2019) 83.
[8] X. Li, P. Li, Z. Wu, D. Luo, H.-Y. Yu, Z.-H. Lu, Review and perspective of materials for flexible solar cells, Mater. Rep.: Energy 1 (2021) 100001.
[9] Y. Du, J. Xu, B. Paul, P. Eklund, Flexible thermoelectric materials and devices, Appl. Mater. Today 12 (2018) 366–388.
[10] Y. Liu, L. Wang, L. Zhao, X. Yu, Y. Zi, Recent progress on flexible nanogenerators toward self-powered systems, InfoMat 2 (2020) 318–340.

[11] M. Cansiz, D. Altinel, G.K. Kurt, Efficiency in RF energy harvesting systems: a comprehensive review, Energy 174 (2019) 292–309.
[12] Y. Wang, H. Wang, J. Xuan, D.Y. Leung, Powering future body sensor network systems: a review of power sources, Biosens. Bioelectron. 166 (2020) 112410.
[13] R. Hahn, S. Wagner, A. Schmitz, H. Reichl, Development of a planar micro fuel cell with thin film and micro patterning technologies, J. Power Sources 131 (2004) 73–78.
[14] K. Jiao, J. Xuan, Q. Du, Z. Bao, B. Xie, B. Wang, et al., Designing the next generation of proton-exchange membrane fuel cells, Nature 595 (2021) 361–369.
[15] Y. Wang, S. Luo, H. Kwok, W. Pan, D. Leung, Microfluidic fuel cells with different types of fuels: a prospective review, Renew. Sustain. Energy Rev. 141 (2021) 110806.
[16] A.J. Bandodkar, J. Wang, Wearable biofuel cells: a review, Electroanalysis 28 (2016) 1188–1200.
[17] X. Huang, L. Zhang, Z. Zhang, S. Guo, H. Shang, Y. Li, et al., Wearable biofuel cells based on the classification of enzyme for high power outputs and lifetimes, Biosens. Bioelectron. 124–125 (2019) 40–52.
[18] S. ul Haque, M. Yasir, S. Cosnier, Recent advancements in the field of flexible/wearable enzyme fuel cells, Biosens. Bioelectron. (2022) 114545.
[19] Y. Duan, H. Liu, W. Zhang, L. Khotseng, Q. Xu, H. Su, Materials, components, assembly and performance of flexible polymer electrolyte membrane fuel cell: a review, J. Power Sources 555 (2023) 232369.
[20] Y. Yang, X. Zhu, Q. Wang, D. Ye, R. Chen, Q. Liao, Towards flexible fuel cells: development, challenge and prospect, Appl. Therm. Eng. 203 (2022) 117937.
[21] J. Wang, N. He, J. Fei, Z. Ma, Z. Ji, Z. Chen, et al., Flexible and wearable fuel cells: a review of configurations and applications, J. Power Sources 551 (2022) 232190.
[22] R. Rosli, A. Sulong, W. Daud, M. Zulkifley, T. Husaini, M. Rosli, et al., A review of high-temperature proton exchange membrane fuel cell (HT-PEMFC) system, Int. J. Hydrogen Energy 42 (2017) 9293–9314.
[23] M. Pan, C. Pan, C. Li, J. Zhao, A review of membranes in proton exchange membrane fuel cells: transport phenomena, performance and durability, Renew. Sustain. Energy Rev. 141 (2021) 110771.
[24] P.C. Okonkwo, O.O. Ige, P.C. Uzoma, W. Emori, A. Benamor, A.M. Abdullah, Platinum degradation mechanisms in proton exchange membrane fuel cell (PEMFC) system: a review, Int. J. Hydrogen Energy 46 (2021) 15850–15865.
[25] M. Chen, C. Zhao, F. Sun, J. Fan, H. Li, H. Wang, Research progress of catalyst layer and interlayer interface structures in membrane electrode assembly (MEA) for proton exchange membrane fuel cell (PEMFC) system, ETransportation 5 (2020) 100075.
[26] F. Lee, M. Ismail, D. Ingham, K. Hughes, L. Ma, S. Lyth, et al., Alternative architectures and materials for PEMFC gas diffusion layers: a review and outlook, Renew. Sustain. Energy Rev. 166 (2022) 112640.
[27] Q. Liu, F. Lan, C. Zeng, J. Chen, J. Wang, A review of proton exchange membrane fuel cell's bipolar plate design and fabrication process, J. Power Sources 538 (2022) 231543.
[28] S. Zhou, L. Fan, G. Zhang, J. Gao, Y. Lu, P. Zhao, et al., A review on proton exchange membrane multi-stack fuel cell systems: architecture, performance, and power management, Appl. Energy 310 (2022) 118555.
[29] W. Daud, R. Rosli, E. Majlan, S. Hamid, R. Mohamed, T. Husaini, PEM fuel cell system control: a review, Renew. Energy 113 (2017) 620–638.
[30] Z. Wang, J. Lv, J. Li, Y. Wang, J. Sun, Fabrication and evaluation of micro-channel array for flexible on-chip PEMFC by new evaluation method and self-made hot embossing system, Int. J. Adv. Des. Manuf. Technol. 108 (2020) 1381–1387.
[31] J. Wheldon, W.-J. Lee, D.-H. Lim, A.B. Broste, M. Bollinger, W.H. Smyrl, High-performance flexible miniature fuel cell, Electrochem. Solid State Lett. 12 (2009) B86.
[32] I. Chang, M.H. Lee, J.-H. Lee, Y.-S. Kim, S.W. Cha, Air-breathing flexible polydimethylsiloxane (PDMS)-based fuel cell, Int. J. Precis. Eng. Manuf. 14 (2013) 501–504.
[33] I. Chang, T. Park, J. Lee, M.H. Lee, S.H. Ko, S.W. Cha, Bendable polymer electrolyte fuel cell using highly flexible Ag nanowire percolation network current collectors, J. Mater. Chem. A 1 (2013) 8541–8546.
[34] I. Chang, T. Park, J. Lee, H.B. Lee, S. Ji, M.H. Lee, et al., Performance enhancement in bendable fuel cell using highly conductive Ag nanowires, Int. J. Hydrogen Energy 39 (2014) 7422–7427.
[35] I. Chang, T. Park, J. Lee, H.B. Lee, S.H. Ko, S.W. Cha, Flexible fuel cell using stiffness-controlled endplate, Int. J. Hydrogen Energy 41 (2016) 6013–6019.
[36] T. Park, I. Chang, J.H. Jung, H.B. Lee, S.H. Ko, R. O'Hayre, et al., Effect of assembly pressure on the performance of a bendable polymer electrolyte fuel cell based on a silver nanowire current collector, Energy 134 (2017) 412–419.
[37] T. Park, I. Chang, H.B. Lee, S.H. Ko, S.W. Cha, Performance variation of bendable polymer electrolyte fuel cell based on Ag nanowire current collector under mixed bending and twisting load, Int. J. Hydrogen Energy 42 (2017) 1884–1890.
[38] H. Yoo, J. Kim, O. Kwon, H. Kim, G.H. Kim, H. Choi, et al., Pre-bent flow-field plates for enhanced performance in flexible polymer electrolyte membrane fuel cells in curved shape, Int. J. Precis. Eng. Manuf. Green Technol. 8 (2021) 869–878.
[39] H. Yoo, O. Kwon, J. Kim, H. Cha, H. Kim, H. Choi, et al., 3D-printed flexible flow-field plates for bendable polymer electrolyte membrane fuel cells, J. Power Sources 532 (2022) 231273.
[40] J. Baek, S-u Moon, J. Kim, H. Yoo, Y.-J. Kwark, T. Park, Development of foldable air-breathing polymer electrolyte membrane fuel cells for power sources of next-generation flexible electronics, J. Power Sources 589 (2024) 233771.
[41] Y.S. Kang, T. Park, S. Jang, M. Choi, S.J. Yoo, S.W. Cha, Repetitive bending test of membrane electrode assembly for bendable polymer electrolyte membrane fuel cell, J. Ind. Eng. Chem. 47 (2017) 323–328.
[42] F. Ning, X. He, Y. Shen, H. Jin, Q. Li, D. Li, et al., Flexible and lightweight fuel cell with high specific power density, ACS Nano 11 (2017) 5982–5991.
[43] Y.S. Kang, P. Won, S.H. Ko, T. Park, S.J. Yoo, Bending-durable membrane-electrode assembly using metal nanowires for bendable polymer electrolyte membrane fuel cell, Energy 172 (2019) 874–880.
[44] F. Ning, Y. Shen, C. Bai, J. Wei, G. Lu, Y. Cui, et al., Critical importance of current collector property to the performance of flexible electrochemical power sources, Chin. Chem. Lett. 30 (2019) 1282–1288.
[45] J. Wei, F. Ning, C. Bai, T. Zhang, G. Lu, H. Wang, et al., An ultra-thin, flexible, low-cost and scalable gas diffusion layer composed of carbon nanotubes for high-performance fuel cells, J. Mater. Chem. A 8 (2020) 5986–5994.
[46] Y. So, H. Yoo, J. Kim, O. Kwon, S. Jeong, H. Choi, et al., Investigation of gas diffusion layers for flexible polymer electrolyte membrane fuel cells, Int. J. Precis. Eng. Manuf. Green Technol. (2023) 1–8.
[47] F.-K. Hsu, M.-S. Lee, C.-C. Lin, Y.-K. Lin, W.-T. Hsu, A flexible portable proton exchange membrane fuel cell, J. Power Sources 219 (2012) 180–187.
[48] T. Park, Y.S. Kang, S. Jang, S.W. Cha, M. Choi, S.J. Yoo, A rollable ultra-light polymer electrolyte membrane fuel cell, NPG Asia Mater. 9 (2017) e384–e.
[49] L. Hakola, A.P. Puerto, A. Vaari, T. Maaninen, A. Kucernak, S. Viik, et al., Anode ink formulation for a fully printed flexible fuel cell stack, Flex. Print. Electron. 5 (2020) 025002.
[50] H. Wang, C. Bai, T. Zhang, J. Wei, Y. Li, F. Ning, et al., Flexible and adaptable fuel cell pack with high energy density realized by a bifunctional catalyst, ACS Appl. Mater. Interfaces 12 (2020) 4473–4481.
[51] T. Ito, K. Kimura, M. Kunimatsu, Characteristics of micro DMFCs array fabricated on flexible polymeric substrate, Electrochem. Commun. 8 (2006) 973–976.
[52] C. Weinmueller, G. Tautschnig, N. Hotz, D. Poulikakos, A flexible direct methanol micro-fuel cell based on a metalized, photosensitive polymer film, J. Power Sources 195 (2010) 3849–3857.
[53] Z. Wu, X. Kuang, L. Liu, X. Wang, A flexible foldable tubular μDMFC for powering wearable devices, J. Microelectromech. Syst. 26 (2017) 1147–1154.
[54] J. Zhu, J. Yu, L. Yin, W. Yang, H. Liu, G. Wang, et al., A flexible micro direct methanol fuel cells array based on FPCB, Energy Convers. Manag. 258 (2022) 115469.
[55] S. Zou, Y. Li, H. Jin, F. Ning, P. Xu, Q. Wen, et al., Highly safe, durable, adaptable, and flexible fuel cell using gel/sponge composite material, Adv. Energy Mater. 12 (2022) 2103178.
[56] S. Sun, M. Zhao, Q. Wang, S. Xue, Q. Huang, N. Yu, et al., Flexible all-solid-state direct methanol fuel cells with high specific power density, Small 19 (2023) 2205835.
[57] L.P. Carneiro, A.M. Pinto, M.G.F. Sales, Development of an innovative flexible paper-based methanol fuel cell (PB-DMFC) sensing platform–Application to sarcosine detection, Chem. Eng. J. 452 (2023) 139563.
[58] X. Li, T. Chao, Y-e Duan, Y. Qu, Y. Liu, Q. Tan, High-performance, stable, and flexible direct methanol fuel cell based on a pre-swelling kalium polyacrylate gel electrolyte and single-atom cathode catalyst, ACS Sustain. Chem. Eng. 9 (2021) 15138–15146.
[59] J. Wang, Z. Pei, J. Liu, M. Hu, Y. Feng, P. Wang, et al., A high-performance flexible direct ethanol fuel cell with drop-and-play function, Nano Energy 65 (2019) 104052.
[60] T. Jiang, J. Gao, Z. Jin, K. Hu, Q. Yuan, H.-J. Qiu, Multicomponent nanoporous Al–Ni–Cu–Pt–Pd–Co as highly stable anode catalysts in a flexible room-temperature pure ethanol–powered solid-state fuel cell, Mater. Today Energy 21 (2021) 100835.
[61] S. Li, J. Wang, X. Lin, G. Xie, Y. Huang, X. Liu, et al., Flexible solid-state direct ethanol fuel cell catalyzed by nanoporous high-entropy Al-Pd-Ni-Cu-Mo anode and spinel (AlMnCo) 3O4 cathode, Adv. Funct. Mater. 31 (2021) 2007129.
[62] Y. Yang, K. Xing, M. Yan, X. Zhu, D. Ye, R. Chen, et al., A potential flexible fuel cell with dual-functional hydrogel based on multi-component crosslinked hybrid polyvinyl alcohol, Energy 265 (2023) 126166.
[63] S.J. Eickhoff, Self-regulating fiber fuel cell. Energy Harvesting and Storage: Materials, Devices, and Applications, International Society for Optics and Photonics, 2010, p. 76830K.
[64] Y. Yang, J. Wang, Y. Zhu, L. Lan, H. Zhang, C. Liu, et al., Fe3C/C nanoparticles encapsulated in N-doped graphene aerogel: an advanced oxygen reduction reaction catalyst for fiber-shaped fuel cells, Int. J. Hydrogen Energy 44 (2019) 18393–18402.
[65] W. Hwang, S. Kim, C.-Y. Ahn, Y.-H. Cho, Y.-E. Sung, Origami-based flexible and simple tubular polymer electrolyte membrane fuel cell stack, ACS Energy Lett. 6 (2021) 3195–3202.
[66] HiroshiNishizeko SatoshiTominaka, TetsuyaOsaka JunMizuno, Bendable fuel cells: on-chip fuel cell on a flexible polymer substrate, Energy Environ. Sci. 2 (2009) 1074–1077.
[67] E. Ortiz-Ortega, M. Gurrola, N. Arjona, J. Ledesma-García, L. Arriaga, A compact and bendable, hook-and-loop tape-based membraneless device for energy conversion, J. Micromech. Microeng. 26 (2016) 124011.
[68] Y. Yang, Y. Xue, H. Zhang, H. Chang, Flexible H2O2 microfluidic fuel cell using graphene/Prussian blue catalyst for high performance, Chem. Eng. J. 369 (2019) 813–817.
[69] T.H. Nguyen, A. Fraiwan, S. Choi, Paper-based batteries: a review, Biosens. Bioelectron. 54 (2014) 640–649.
[70] F. Sharifi, S. Ghobadian, F.R. Cavalcanti, N. Hashemi, Paper-based devices for energy applications, Renew. Sustain. Energy Rev. 52 (2015) 1453–1472.
[71] B. Yao, J. Zhang, T. Kou, Y. Song, T. Liu, Y. Li, Paper-based electrodes for flexible energy storage devices, Adv. Sci. 4 (2017) 1700107.

[72] J. Esquivel, F. Del Campo, J.G. De La Fuente, S. Rojas, N. Sabate, Microfluidic fuel cells on paper: meeting the power needs of next generation lateral flow devices, Energy Environ. Sci. 7 (2014) 1744–1749.

[73] R.K. Arun, S. Halder, N. Chanda, S. Chakraborty, A paper based self-pumping and self-breathing fuel cell using pencil stroked graphite electrodes, Lab Chip 14 (2014) 1661–1664.

[74] L.T. Rao, S.K. Dubey, A. Javed, S. Goel, Statistical performance analysis and robust design of paper microfluidic membraneless fuel cell with pencil graphite electrodes, J. Electrochem. Energy Convers. Storage 17 (2020) 031015.

[75] L. Tata Rao, P. Rewatkar, S.K. Dubey, A. Javed, S. Goel, Performance optimization of microfluidic paper fuel-cell with varying cellulose fiber papers as absorbent pad, Int. J. Energy Res. 44 (2020) 3893–3904.

[76] S. Lal, V.M. Janardhanan, M. Deepa, A. Sagar, K.C. Sahu, Low cost environmentally benign porous paper based fuel cells for micro-nano systems, J. Electrochem. Soc. 162 (2015) F1402.

[77] T.S. Copenhaver, K.H. Purohit, K. Domalaon, L. Pham, B.J. Burgess, N. Manorothkul, et al., A microfluidic direct formate fuel cell on paper, Electrophoresis 36 (2015) 1825–1829.

[78] V. Galvan, K. Domalaon, C. Tang, S. Sotez, A. Mendez, M. Jalali-Heravi, et al., An improved alkaline direct formate paper microfluidic fuel cell, Electrophoresis 37 (2016) 504–510.

[79] J. Ma, C. Zhang, F. Xi, W. Chen, K. Jiao, Q. Du, et al., Experimental study on the influence of environment conditions on the performance of paper-based microfluidic fuel cell, Appl. Therm. Eng. 219 (2023) 119487.

[80] L. Li, Y. He, Q. Xu, T. Liu, S. Bei, K. Zheng, et al., A paper-based self-pumping microfluidic fuel cell stack with a novel vertical structure, Int. J. Energy Res. 46 (2022) 8389–8397.

[81] Z. Liu, J. Ma, K. Jiao, Q. Du, F. Bai, Fabrication of high power density paper-based microfluidic fuel cell using a stepped catalyst layer, Biosens. Bioelectron. X 14 (2023) 100345.

[82] K.H. Purohit, S. Emrani, S. Rodriguez, S.-S. Liaw, L. Pham, V. Galvan, et al., A microfluidic galvanic cell on a single layer of paper, J. Power Sources 318 (2016) 163–169.

[83] L.-L. Shen, G.-R. Zhang, T. Venter, M. Biesalski, B.J. Etzold, Towards best practices for improving paper-based microfluidic fuel cells, Electrochim. Acta 298 (2019) 389–399.

[84] W. Wang, L.-L. Shen, H. Yu, W. Xu, J. Wang, C. Yong, et al., Solar-Boosted paper-based microfluidic fuel cells for miniaturized power sources, Adv. Mater. Technol. 7 (2022) 2200154.

[85] S. Chandra, S. Lal, V.M. Janardhanan, K.C. Sahu, M. Deepa, Ethanol based fuel cell on paper support, J. Power Sources 396 (2018) 725–733.

[86] A.L.D. Lima, P.M. Rocha, A.C. Silva, J. Alves Fernandes, C.A. Martins, Interchangeable biomass fuels for paper-based microfluidic fuel cells: finding their power density limits, ACS Appl. Mater. Interfaces 15 (2023) 11895–11905.

[87] V. Pasala, K. Ramanujam, Flexible paper-based borohydride-vanadium fuel cell for powering micro-nanosystems, Ionics 23 (2017) 1811–1817.

[88] D.-G. Jung, Y. Ahn, Microfabricated paper-based vanadium co-laminar flow fuel cell, J. Power Sources 451 (2020) 227801.

[89] I. Chino, O. Muneeb, E. Do, V. Ho, J.L. Haan, A paper microfluidic fuel cell powered by urea, J. Power Sources 396 (2018) 710–714.

[90] S. Luo, W. Pan, Y. Wang, X. Zhao, K. Wah Leong, D.Y.C. Leung, High-performance H2O2 paper fuel cell boosted via electrolyte toning and radical generation, Appl. Energy 323 (2022) 119610.

[91] R. Verma, S. Lal, M. Deepa, V.M. Janardhanan, K.C. Sahu, Sodium percarbonate based, mixed-media fuel cells supported on paper with gold/nickel oxide catalysts, Chemelectrochem 4 (2017) 310–319.

[92] S. Lal, M. Deepa, V.M. Janardhanan, K.C. Sahu, Paper based hydrazine monohydrate fuel cells with Cu and C composite catalysts, Electrochim. Acta 232 (2017) 262–270.

[93] S.M.M. Ehteshami, M. Asadnia, S.N. Tan, S.H. Chan, Based membraneless hydrogen peroxide fuel cell prepared by micro-fabrication, J. Power Sources 301 (2016) 392–395.

[94] X. Yan, A. Xu, L. Zeng, P. Gao, T. Zhao, A paper-based microfluidic fuel cell with hydrogen peroxide as fuel and oxidant, Energy Technol. 6 (2018) 140–143.

[95] R.K. Arun, V. Gupta, P. Singh, G. Biswas, N. Chanda, Selection of graphite pencil grades for the design of suitable electrodes for stacking multiple single-inlet paper-pencil fuel cells, ChemistrySelect 4 (2019) 152–159.

[96] S. Luo, Y. Wang, T.C. Kong, W. Pan, X. Zhao, D.Y.C. Leung, Flexible direct formate paper fuel cells with high performance and great durability, J. Power Sources 490 (2021) 229526.

[97] J. Esquivel, J. Buser, C. Lim, C. Domínguez, S. Rojas, P. Yager, et al., Single-use paper-based hydrogen fuel cells for point-of-care diagnostic applications, J. Power Sources 342 (2017) 442–451.

[98] Y. Wang, H.Y. Kwok, Y. Zhang, W. Pan, H. Zhang, X. Lu, et al., A flexible paper-based hydrogen fuel cell for small power applications, Int. J. Hydrogen Energy 44 (2019) 29680–29691.

[99] J. Ji, S.M. Jeon, Y. Chung, Y. Kwon, Paper-based flexible membraneless fuel cells using vitamins as both anodic catalyst and fuel, Int. J. Energy Res. 46 (2022) 15781–15792.

[100] M. Asadnia, S.M.M. Ehteshami, S.H. Chan, M.E. Warkiani, Development of a fiber-based membraneless hydrogen peroxide fuel cell, RSC Adv. 7 (2017) 40755–40760.

[101] N.H. Park, J. Kim, Y. Ahn, Fabric-based self-pumping, single-stream microfluidic fuel cell, Electrochim. Acta 446 (2023) 142106.

[102] K. Domalaon, C. Tang, A. Mendez, F. Bernal, K. Purohit, L. Pham, et al., Fabric-based alkaline direct formate microfluidic fuel cells, Electrophoresis 38 (2017) 1224–1231.

[103] Z. Liu, D. Ye, X. Zhu, S. Wang, R. Chen, Y. Yang, et al., A self-pumping microfluidic fuel cell powered by formate with Pd coated carbon cloth electrodes, J. Power Sources 490 (2021) 229553.

[104] Q. Zhai, Y. Liu, R. Wang, Y. Wang, Q. Lyu, S. Gong, et al., Intrinsically stretchable fuel cell based on enokitake-like standing gold nanowires, Adv. Energy Mater. 10 (2020) 1903512.

[105] S. Gong, S. Du, J. Kong, Q. Zhai, F. Lin, S. Liu, et al., Skin-like stretchable fuel cell based on gold-nanowire-impregnated porous polymer scaffolds, Small 16 (2020) 2003269.

[106] Y. Lu, Z. Yong, S. Gong, Q. Shi, F. Lin, Q. Zhai, et al., Pd-conformally coated, one-end-embedded gold nanowire percolation network for intrinsically stretchable, epidermal tattoo fuel cell, Biosens. Bioelectron. 221 (2023) 114924.

[107] Z. Liu, D. Ye, R. Chen, B. Zhang, X. Zhu, J. Li, et al., A woven thread-based microfluidic fuel cell with graphite rod electrodes, Int. J. Hydrogen Energy 43 (2018) 22467–22473.

[108] R. Wu, D. Ye, R. Chen, B. Zhang, X. Zhu, H. Guo, et al., A membraneless microfluidic fuel cell with continuous multistream flow through cotton threads, Int. J. Energy Res. 44 (2020) 2243–2251.

[109] S. Wang, D. Ye, Z. Liu, R. Chen, X. Zhu, B. Zhang, et al., A direct formate microfluidic fuel cell with cotton thread-based electrodes, Int. J. Hydrogen Energy 45 (2020) 27665–27674.

[110] Z. Liu, D. Ye, R. Chen, B. Zhang, X. Zhu, Q. Liao, A dual-functional three-dimensional herringbone-like electrode for a membraneless microfluidic fuel cell, J. Power Sources 438 (2019) 227058.

[111] Z. Liu, D. Ye, X. Zhu, S. Wang, Y. Zou, L. Lan, et al., ZIF-67-derived Co nanoparticles embedded in N-doped porous carbon composite interconnected by MWCNTs as highly efficient ORR electrocatalysts for a flexible direct formate fuel cell, Chem. Eng. J. 432 (2022) 134192.

[112] Z. Liu, D. Ye, S. Wang, X. Zhu, R. Chen, Q. Liao, Single-stream H2O2 membraneless microfluidic fuel cell and its application as a self-powered electrochemical sensor, Ind. Eng. Chem. Res. 59 (2020) 15447–15453.

[113] X. Zhou, X. Zheng, J. Xu, S. Dai, X. Wang, X. Hu, et al., Wire-Shaped and membrane-free fuel cell based on biscrolled carbon nanotube yarn, Energy Technol. 7 (2019) 1900122.

[114] S. Wang, D. Ye, Z. Liu, X. Zhu, R. Chen, Q. Liao, et al., A flexible on-fiber H2O2 microfluidic fuel cell with high power density, Int. J. Hydrogen Energy 47 (7) (2022) 4793–4803.

[115] Y. Fukushi, S. Koide, R. Ikoma, W. Akatsuka, S. Tsujimura, Y. Nishioka, Fabrication and characterization of glucose fuel cells with a microchannel fabricated on flexible polyimide film, J. Photopolym. Sci. Technol. 26 (2013) 303–308.

[116] Y. Fujimagari, Y. Fukushi, Y. Nishioka, Stretchable biofuel cells with silver nanowiring on a polydimethylsiloxane substrate, J. Photopolym. Sci. Technol. 28 (2015) 357–361.

[117] D. Pankratov, R. Sundberg, J. Sotres, I. Maximov, M. Graczyk, D.B. Suyatin, et al., Transparent and flexible, nanostructured and mediatorless glucose/oxygen enzymatic fuel cells, J. Power Sources 294 (2015) 501–506.

[118] M. Falk, V. Andoralov, Z. Blum, J. Sotres, D.B. Suyatin, T. Ruzgas, et al., Biofuel cell as a power source for electronic contact lenses, Biosens. Bioelectron. 37 (2012) 38–45.

[119] M. Falk, V. Andoralov, M. Silow, M.D. Toscano, S. Shleev, Miniature biofuel cell as a potential power source for glucose-sensing contact lenses, Anal. Chem. 85 (2013) 6342–6348.

[120] X. Xiao, T. Siepenkoetter, P.O. Conghaile, Dn Leech, E. Magner, Nanoporous gold-based biofuel cells on contact lenses, ACS Appl. Mater. Interfaces 10 (2018) 7107–7116.

[121] R.C. Reid, S.R. Jones, D.P. Hickey, S.D. Minteer, B.K. Gale, Modeling carbon nanotube connectivity and surface activity in a contact lens biofuel cell, Electrochim. Acta 203 (2016) 30–40.

[122] R.C. Reid, S.D. Minteer, B.K. Gale, Contact lens biofuel cell tested in a synthetic tear solution, Biosens. Bioelectron. 68 (2015) 142–148.

[123] W. Jia, G. Valdés-Ramírez, A.J. Bandodkar, J.R. Windmiller, J. Wang, Epidermal biofuel cells: energy harvesting from human perspiration, Angew. Chem. Int. Ed. 52 (2013) 7233–7236.

[124] A.J. Bandodkar, J.-M. You, N.-H. Kim, Y. Gu, R. Kumar, A.V. Mohan, et al., Soft, stretchable, high power density electronic skin-based biofuel cells for scavenging energy from human sweat, Energy Environ. Sci. 10 (2017) 1581–1589.

[125] X. Chen, L. Yin, J. Lv, A.J. Gross, M. Le, N.G. Gutierrez, et al., Stretchable and flexible buckypaper-based lactate biofuel cell for wearable electronics, Adv. Funct. Mater. 29 (2019) 1905785.

[126] M. Sun, Y. Gu, X. Pei, J. Wang, J. Liu, C. Ma, et al., A flexible and wearable epidermal ethanol biofuel cell for on-body and real-time bioenergy harvesting from human sweat, Nano Energy 86 (2021) 106061.

[127] C.H. Kwon, S.-H. Lee, Y.-B. Choi, J.A. Lee, S.H. Kim, H.-H. Kim, et al., High-power biofuel cell textiles from woven biscrolled carbon nanotube yarns, Nat. Commun. 5 (2014) 3928.

[128] W. Jia, X. Wang, S. Imani, A.J. Bandodkar, J. Ramírez, P.P. Mercier, et al., Wearable textile biofuel cells for powering electronics, J. Mater. Chem. A 2 (2014) 18184–18189.

[129] I. Jeerapan, J.R. Sempionatto, A. Pavinatto, J.-M. You, J. Wang, Stretchable biofuel cells as wearable textile-based self-powered sensors, J. Mater. Chem. A 4 (2016) 18342–18353.

[130] C. Wang, E. Shim, H.-K. Chang, N. Lee, H.R. Kim, J. Park, Sustainable and high-power wearable glucose biofuel cell using long-term and high-speed flow in sportswear fabrics, Biosens. Bioelectron. 169 (2020) 112652.
[131] I. Shitanda, Y. Morigayama, R. Iwashita, H. Goto, T. Aikawa, T. Mikawa, et al., Paper-based lactate biofuel cell array with high power output, J. Power Sources 489 (2021) 229533.
[132] I. Shitanda, Y. Fujimura, T. Takarada, R. Suzuki, T. Aikawa, M. Itagaki, et al., Self-powered diaper sensor with wireless transmitter powered by paper-based biofuel cell with urine glucose as fuel, ACS Sens. 6 (2021) 3409–3415.
[133] Y. Ogawa, Y. Takai, Y. Kato, H. Kai, T. Miyake, M. Nishizawa, Stretchable biofuel cell with enzyme-modified conductive textiles, Biosens. Bioelectron. 74 (2015) 947–952.
[134] Y. Hui, X. Ma, F. Qu, Flexible glucose/oxygen enzymatic biofuel cells based on three-dimensional gold-coated nickel foam, J. Solid State Electrochem. 23 (2019) 169–178.
[135] S. Yin, Z. Jin, T. Miyake, Wearable high-powered biofuel cells using enzyme/carbon nanotube composite fibers on textile cloth, Biosens. Bioelectron. 141 (2019) 111471.
[136] X. Kong, P. Gai, L. Ge, F. Li, Laser-scribed N-doped graphene for integrated flexible enzymatic biofuel cells, ACS Sustain. Chem. Eng. 8 (2020) 12437–12442.
[137] R. Suzuki, I. Shitanda, T. Aikawa, T. Tojo, T. Kondo, S. Tsujimura, et al., Wearable glucose/oxygen biofuel cell fabricated using modified aminoferrocene and flavin adenine dinucleotide-dependent glucose dehydrogenase on Poly (glycidyl methacrylate)-grafted MgO-templated Carbon, J. Power Sources 479 (2020) 228807.
[138] Z. Chen, Y. Yao, T. Lv, Y. Yang, Y. Liu, T. Chen, Flexible and stretchable enzymatic biofuel cell with high performance enabled by textile electrodes and polymer hydrogel electrolyte, Nano Lett. 22 (2022) 196–202.
[139] Y. Yang, Y. Su, X. Zhu, D. Ye, R. Chen, Q. Liao, Flexible enzymatic biofuel cell based on 1, 4-naphthoquinone/MWCNT-Modified bio-anode and polyvinyl alcohol hydrogel electrolyte, Biosens. Bioelectron. 198 (2022) 113833.
[140] C. Siu, M. Chiao, A microfabricated PDMS microbial fuel cell, J. Microelectromech. Syst. 17 (2008) 1329–1341.
[141] J.E. Mink, R.M. Qaisi, M.M. Hussain, Graphene-based flexible micrometer-sized microbial fuel cell, Energy Technol. 1 (2013) 648–652.
[142] A. Fraiwan, S. Mukherjee, S. Sundermier, H.-S. Lee, S. Choi, A paper-based microbial fuel cell: instant battery for disposable diagnostic devices, Biosens. Bioelectron. 49 (2013) 410–414.
[143] A. Fraiwan, H. Lee, S. Choi, A multianode paper-based microbial fuel cell: a potential power source for disposable biosensors, IEEE Sensor. J. 14 (2014) 3385–3390.
[144] R. Veerubhotla, A. Bandopadhyay, D. Das, S. Chakraborty, Instant power generation from an air-breathing paper and pencil based bacterial bio-fuel cell, Lab Chip 15 (2015) 2580–2583.
[145] A. Fraiwan, S. Choi, A stackable, two-chambered, paper-based microbial fuel cell, Biosens. Bioelectron. 83 (2016) 27–32.
[146] R. Veerubhotla, D. Das, D. Pradhan, A flexible and disposable battery powered by bacteria using eyeliner coated paper electrodes, Biosens. Bioelectron. 94 (2017) 464–470.
[147] M. Mohammadifar, J. Zhang, I. Yazgan, O. Sadik, S. Choi, Power-on-paper: origami-inspired fabrication of 3-D microbial fuel cells, Renew. Energy 118 (2018) 695–700.
[148] U. Jayapiriya, S. Goel, Influence of cellulose separators in coin-sized 3D printed paper-based microbial fuel cells, Sustain. Energy Technol. Assessments 47 (2021) 101535.
[149] S. Pang, Y. Gao, S. Choi, Flexible and stretchable microbial fuel cells with modified conductive and hydrophilic textile, Biosens. Bioelectron. 100 (2018) 504–511.
[150] S. Pang, Y. Gao, S. Choi, Flexible and stretchable biobatteries: monolithic integration of Membrane-Free microbial fuel cells in a single textile layer, Adv. Energy Mater. 8 (2018) 1702261.
[151] J. Ryu, Y. Gao, J.H. Cho, S. Choi, Horizontally structured microbial fuel cells in yarns and woven fabrics for wearable bioenergy harvesting, J. Power Sources 484 (2021) 229271.
[152] K.-B. Pu, T.-T. Li, J.-Y. Gao, Q.-Y. Chen, K. Guo, M. Zhou, et al., Floating flexible microbial fuel cells for electricity generation and municipal wastewater treatment, Sep. Purif. Technol. 300 (2022) 121915.
[153] M. Taghavi, J. Greenman, L. Beccai, V. Mattoli, B. Mazzolai, C. Melhuish, et al., High-performance, totally flexible, tubular microbial fuel cell, Chemelectrochem 1 (2014) 1994–1999.
[154] M. Yu, X. Cheng, Y. Zeng, Z. Wang, Y. Tong, X. Lu, et al., Dual-doped molybdenum trioxide nanowires: a bifunctional anode for fiber-shaped asymmetric supercapacitors and microbial fuel cells, Angew. Chem. 128 (2016) 6874–6878.
[155] H.J. Cho, G.M. Choi, Fabrication and characterization of Ni-supported solid oxide fuel cell, Solid State Ionics 180 (2009) 792–795.
[156] H.J. Cho, K.J. Kim, Y.M. Park, G.M. Choi, Flexible solid oxide fuel cells supported on thin and porous metal, Int. J. Hydrogen Energy 41 (2016) 9577–9584.
[157] O.S. Jeon, H.J. Hwang, O. Chan Kwon, J.G. Lee, Y.G. Shul, Next-generation flexible solid oxide fuel cells with high thermomechanical stability, J. Mater. Chem. A 6 (2018) 18018–18024.
[158] B.-R. Won, Y.H. Kim, S. Jo, J-h Myung, Highly flexible solid oxide fuel cells using phase-controlled electrolyte support, J. Eur. Ceram. Soc. 42 (2022) 5813–5819.
[159] G. Lui, G. Jiang, J. Lenos, E. Lin, M. Fowler, A. Yu, et al., Advanced biowaste-based flexible photocatalytic fuel cell as a green wearable power generator, Adv. Mater. Technol. 2 (2017) 1600191.
[160] Z. Yang, M. Zhu, Y. Niu, E. Kozliak, B. Yao, Y. Zhang, et al., A graphene-based coaxial fibrous photofuel cell powered by mine gas, Adv. Funct. Mater. 29 (2019) 1906813.
[161] L. Xiong, G. Liu, H. Fu, M. Wang, J. Kim, W. Yang, et al., Wearable eutectic gallium-indium liquid fuel cells, Energy Convers. Manag. 247 (2021) 114729.